Learning How to Smile: Can Rational Learning Explain the Predictable Dynamics in the Implied Volatility Surface?

Alejandro Bernales and Massimo Guidolin*

Abstract

We develop a general equilibrium asset pricing model under rational learning to explain the puzzling and yet unexplained predictable dynamics observable in option prices. In our model, the fundamental dividend growth rate is unknown and subject to breaks, where time periods between breaks follow a memory-less stochastic process. Immediately after a break there is insufficient information to price option contracts accurately. However, as new information arrives a representative Bayesian agent recursively learns about the parameters of the process followed by fundamentals. We show that learning makes beliefs time-varying in ways that induce large and dynamic premiums in option prices and their implied volatilities. In addition, we find that learning generates different dynamic effects across option contracts with different strike prices and maturities, which induce rich and realistic movements in the volatility surface implicit in option prices. Moreover, similarly to the predictability features observable from option market data, learning yields statistically strong predictable dynamics in option prices.

* Alejandro Bernales is at la Banque de France (Financial Economics Research Service, DGEI-DEMFI-RECFIN), email: alejandro.bernales@banque-france.fr. Massimo Guidolin is at Manchester Business School, University of Manchester, email: massimo.guidolin@mbs.ac.uk. The authors would like to thank Michael Brennan, Christian Hellwig, Jean-Stéphane Mésonnier, Gaetano Gaballo, Alex Taylor, Stuart Hyde, and Mario Cerrato for their comments on earlier versions of this paper. The authors are very grateful for the computational resources proportioned by the computing grids MACE and MAN2 at the University of Manchester and especially for the useful help from Simon Hood and Michael Croucher in running algorithms in the grids (MACE is part of the Mechanical, Aerospace & Civil Engineering School, while MAN2 is part of the British North West Grid).

Learning How to Smile: Can Rational Learning Explain the Predictable Dynamics in the Implied Volatility Surface?

Abstract

We develop a general equilibrium asset pricing model under rational learning to explain the puzzling and yet unexplained predictable dynamics observable in option prices. In our model, the fundamental dividend growth rate is unknown and subject to breaks, where time periods between breaks follow a memory-less stochastic process. Immediately after a break there is insufficient information to price option contracts accurately. However, as new information arrives a representative Bayesian agent recursively learns about the parameters of the process followed by fundamentals. We show that learning makes beliefs time-varying in ways that induce large and dynamic premiums in option prices and their implied volatilities. In addition, we find that learning generates different dynamic effects across option contracts with different strike prices and maturities, which induce rich and realistic movements in the volatility surface implicit in option prices. Moreover, similarly to the predictability features observable from option market data, learning yields statistically strong predictable dynamics in option prices.

1 Introduction

Contrary to the constant volatility assumption of the Black and Scholes (1973) model, the volatilities implicit in option contracts change over time. Moreover, it is well known that statistically strong predictability patterns in implied volatilities and option prices exist (e.g., Harvey and Whaley (1992), Heston and Nandi (2000), Gonçalves and Guidolin (2006), Konstantinidi *et al*. (2008), and Christoffersen *et al.* (2009)). Additionally, and equally in contrast with Black and Scholes' (1973) assumptions, the volatilities implicit in option contracts written on the same underlying asset differ across strike prices and expiration dates; these cross-sectional differences in implied volatilities are known as the implied volatility surface, henceforth *IVS*.[1] Furthermore, and similarly to the behaviour of the implied volatility of a single option contract, there is evidence of predictable dynamics in the shape characteristics of the *IVS* (e.g., Gonçalves and Guidolin (2006) and Chalamandaris and Tsekrekos (2010)). In spite of this diffuse and compelling evidence of dynamics in the volatilities implicit in traded options, there has been a limited number of efforts in the financial economics literature aimed at developing equilibrium pricing models that may generate from first principles such ubiquitous patterns of dynamic predictability (i.e. from simple and generally accepted assumptions concerning preferences and the stochastic process of fundamentals driving asset prices). The main goal of our research is to fill this gap by presenting a rather standard and yet powerful equilibrium model in which the investors' rational learning process explains the predictable dynamics in option prices and corresponding implied volatilities.

In particular, we develop a discrete-time endowment economy in which a representative agent has to price a risk-free, one-period bond, a stock, and a set of option contracts with different strike prices and expiration dates. The stock pays out an infinite stream of real dividends which evolve according to a geometric random walk; although, the mean dividend growth rate, g_t, is subject to breaks where time periods between breaks follow a memory-less stochastic process. In the case in which a break takes place, the new mean dividend growth rate is drawn from a continuous

[1] See, e.g. Rubinstein (1985), Dumas *et al.* (1998), and Das and Sundaram (1999)).

univariate density $g_{t+1} \sim G(\cdot)$ defined on the support $[g_d, g_u]$. However, g_t is unknown by the agent, who recursively obtains incomplete information about the mean growth rate by observing independently distributed although noisy daily dividend realizations. The agent efficiently uses these signals following a rational Bayesian learning process. Immediately after a break, historical information is scarce which induce uncertain reliability; and thus drastic revisions of the beliefs concerning the new post-break value of g_t are likely. These initial large updates in beliefs gradually decline as the agent endogenously learns as new information arrives, and as long as no new stochastic breaks occur. Nevertheless, learning never disappears completely even asymptotically because its strength is destined to be revived once again after a new break hits the mean growth rate. Therefore, breaks in the mean growth rate induce two main effects on all assets. First, breaks in g_t impact the stochastic evolution of future dividends, affecting the pricing of all securities directly. Second, breaks modify the quantity and reliability of the information that the agent holds regarding the mean dividend growth rate g_t and hence breaks change the speed and intensity with which she updates her beliefs. Moreover, given that the learning process followed by the agent produces dynamics in her beliefs, this process of recursive belief adjustments is responsible for corresponding and highly non-linear dynamics in options prices and particularly in the associated *IVS*.

Financial markets and the economy are subject to continuous changes that force investors to an ever progressing process of learning on the fundamentals. There is a vast literature reporting breaks in economic fundamentals, such as in the parameters of the dividend process and in the real GDP growth (e.g., Bai et al. (1998), Timmermann (2001), and Granger and Hyung (2004)). Breaks in fundamentals could be due to permanent technological innovations, shifts in tax codes, shifts in monetary policy, or shifts in stock market participation, among other possibilities. However, breaks in economic fundamentals will require that agents optimally follow a learning process as they need to understand the new market conditions. Learning is a skill inherent in all human beings; and hence investors in all markets worldwide are deeply affected by ongoing cognitive outcomes which result from incessant economic transformations. Therefore, our study proposes a simple and yet powerful model (i.e.

for its consequences on our understanding of the dynamic process followed by option prices and implied volatilities) that allows us to show that such learning process makes investors' beliefs time-varying, which affects dynamically the pricing process of options.

Through an extensive set of simulations that adopt the same rules as in established option markets concerning the origination of tradable option contracts in terms of their strike prices, expiration dates, and listing and delisting policies, we show that the learning process induces dynamic patterns in option prices and implied volatilities that are consistent with what is commonly reported in the empirical literature. We find that learning produces different dynamics in the implied volatilities across strike prices and time-to-maturities and thus induces movements in the *IVS* shape. We also show that learning induces serial correlations and volatility clustering in implied volatilities as well as in the slope and curvature of the *IVS,* in a similar way to the behaviour of option contracts observable in the market.[2] We compare the results of our simulations, using multiple predictability measures, with option market data concerning S&P 500 index options and a number of equity options traded in the United States, and we show that our learning model generates to a large extent the same predictable feature described by traded option prices.

The closest papers related to ours are David and Veronesi (2002), Guidolin and Timmermann (2003), and Shaliastovich (2008). These studies explore the effects of learning on option prices, measured at a certain point in time (i.e. performing a static analysis), to explain the different implied volatilities across strike prices and maturity dates which define the *IVS*. These studies show that learning induces asymmetric slopes and curvatures in the *IVS*, which is a result also obtained by our model. David and Veronesi (2002) introduce a model in which the dividend drift follows a two-state regime switching process. In their model, the investors' uncertainty about the current state of the economy induces cross-sectional implied volatility skews and systematic shapes in the term-structure of the *IVS*. Guidolin and Timmermann (2003) present a

[2] Predictability patterns in the level, slopes, and curvatures of the *IVS* have been already reported in empirical studies using S&P 500 index options (e.g., Gonçalves and Guidolin (2006)) and equity options (e.g., Bernales and Guidolin (2011)).

discrete-time equilibrium model in which the mean dividend growth rate evolves between two states in a binomial lattice with an unknown but recursively updated state probability. However, in Guidolin and Timmermann (2003) learning effects vanish asymptotically when time goes to infinity because investors achieve a complete knowledge of the unknown state probability.[3] Shaliastovich (2008) introduce a discrete-time long-run risk type model in which the unobservable consumption growth rate has to be learned by a recency-biased updating procedure. In Shaliastovich (2008) the expected consumption growth and its uncertainty are time-varying, while uncertainty is subject to jumps. However, David and Veronesi (2002), Guidolin and Timmermann (2003), and Shaliastovich (2008) do not explore the time dimension of the learning process to understand the predictable dynamics in option prices such as the autocorrelation of implied volatilities, the volatility clustering of implied volatilities, or the predictability patterns in slopes and curvatures of the *IVS* as in our study.

Furthermore, there are some additional studies that are related to our research, although they do not specifically investigate learning effects on predictable option price dynamics. Our research has links to studies that examine structural breaks in economic fundamentals in relation to the effects of learning on stock prices and their return process (e.g. Timmermann (2001), and Pastor and Stambaugh (2001)). Furthermore, Lettau and Van Nieuwerburgh (2008) show that the return predictability puzzle can be also explained by breaks in economic fundamentals. They show that in-sample financial ratios and future returns are significantly related; however, in real time this relationship cannot be exploited due to breaks. Lettau and Van Nieuwerburgh (2008) find that the return predictability is affected mainly by the uncertainty induced in the estimation of the new economic fundamental value after breaks, whereas the uncertainty generated by the detection of breaking dates is not critical. Ederington and Lee (1996) and Beber and Brandt (2006, 2009) show that macroeconomic events or news at both expected and unexpected times increase implied volatilities, while implied volatilities decline when uncertainty is resolved.

[3] Although Guidolin and Timmermann (2003) perform a dynamic analysis, they only examine the weekly fit of their model over time. Therefore, they do not study specifically whether their model may generate predictable dynamics in option prices and their *IVS*.

Donders *et al.* (2000), Dubinsky and Johannes (2006), and Ni *et al.* (2008) present similar results to Ederington and Lee (1996) and Beber and Brandt (2006, 2009), though they study the effects of earnings announcement dates on implied volatilities.[4]

We contribute to the body of knowledge on understanding the predictability patterns in option prices through an investors' learning process. To the best of our knowledge there is no literature in which the predictable dynamics in implied volatilities or the predictable movements of the *IVS* shapes have been explicitly connected to preferences and beliefs, as we instead do through our dynamic asset pricing model under rational learning. Therefore, the focus of our research on the role played by learning and its effects on the dynamic properties of option prices appears novel and distinctive. The study is organized as follows. Section 2 presents the model, and section 3 describes the simulations and results. Concluding remarks appear in section 4.

2 The Model

2.1 Option Pricing under Breaks and Complete Information

We consider a representative agent discrete-time endowment economy as in Lucas (1978). This economy contains three types of assets: a one-period zero-coupon default free bond, B_t, in zero net supply; a stock with net supply normalized at one, S_t; and a set of call option contracts, $Call_t(K,\tau)$, which are European-style with underlying asset S_t, strike price K, and time-to-maturity τ. The stock pays out infinite real dividends; however the mean dividend growth rate, g_t, presents breaks. The time periods between breaks follow a memory-less geometric process with parameter π; and thus the number of breaks in a given period follows a Bernoulli trial.[5] We assume

[4] See also Patell and Wolfson (1979, 1981), and Whaley and Cheung (1982) in relation to the impact of earning announcements on option prices.

[5] Shaliastovich (2008) uses a continuous-time Poisson process in his discrete-time learning model to describe jumps in the uncertainty over time, and thus time periods between jumps follow a memory-less exponential process which is also in continuous-time. These kinds of setups are common in the literature. However, we prefer to be consistent with our discrete-time model; and thus we use the

that when a break happens, the new mean dividend growth rate is obtained from a continuous univariate density $g_{t+1} \sim G(\cdot)$ defined on the support $[g_d, g_u]$. In addition, dividends evolve according to a geometric random walk process with volatility σ and drift μ_{t+1}:

$$\ln\left(\frac{D_{t+1}}{D_t}\right) = \mu_{t+1} + \sigma\varepsilon_{t+1} \tag{1}$$

in which the innovation term, ε_{t+1}, is homoscedastic and serially uncorrelated; however, μ_{t+1} changes over time since it is related to g_{t+1} by $1 + g_{t+1} = \exp(\mu_{t+1} + \sigma^2/2)$. [6]

We consider a perfect capital market with the objective of pricing assets. There are no taxes, no transaction costs, unlimited short sales possibilities, perfect liquidity, and no borrowing and lending constraints. The representative agent has a power utility at time t:

$$u(C_t) = \begin{cases} \dfrac{C_t^{1-\alpha} - 1}{1-\alpha} & \alpha \geq 0 \\ \ln C_t & \alpha = 1 \end{cases} \tag{2}$$

where C_t is the real consumption, while α corresponds to the coefficient of relative risk aversion. We assume that dividends represent the unique source of income, which are perishable and consumed when they are received at any time $t + k$ (i.e. $C_{t+k} = D_{t+k}$). Therefore and depending on budget constraints, the representative agent maximizes her discount value of expected future utilities choosing assets' holdings:

'discrete-time' versions of the Poisson and exponential processes which are the Bernoulli trial and the memory-less geometric process, respectively.

[6] Despite the fact we could include in our model the assumption in which the volatility of the dividend random walk process changes over time as g_t, we assume that σ is constant to obtain the simplest setting to analyse the impacts of learning on the dynamics of option prices. Through this setup we isolate the sources of learning to one parameter which has to be learned. Furthermore, as in our model, Timmermann (1996, 2001) shows in stock prices that the investors' learning regarding only the mean dividend growth rate induce excess volatility and volatility clustering in stock returns, even though the volatility of the dividend random walk process is invariable. Similarly to Timmermann (1996, 2001), our hypothesis is that learning should also affect dynamically option prices and thus it should be the reason for predictability pattern in option prices and implied volatilities.

$$\max_{\{D_{t+k}, w^S_{t+k}, w^B_{t+k}\}} E_t\left[\sum_{k=0}^{\infty} \beta^k u(D_{t+k})\right]$$
$$\text{s.t.} \quad C_{t+k} + w^S_{t+k} S_{t+k} + w^B_{t+k} B_{t+k} \leq w^S_{t+k-1}(S_{t+k-1} + D_{t+k-1}) + w^B_{t+k-1} \tag{3}$$

with $\beta = 1/(1+\rho)$, ρ is the impatience rate, and w^S_{t+k} (w^B_{t+k}) is the quantity of stocks (bonds) in her portfolio. Since call option contracts are redundant assets, option holdings are not considered in the agent's maximization; and hence they do not affect stock and bond prices. Consequently, Euler equations are obtained for the stock and bond by standard dynamic programming methods:

$$S_t = \mathrm{E}_t\left[\beta\left(\frac{D_{t+1}}{D_t}\right)^{-\alpha}(S_{t+1} + D_{t+1})\right] \tag{4}$$

$$B_t = \mathrm{E}_t\left[\beta\left(\frac{D_{t+1}}{D_t}\right)^{-\alpha}\right] \tag{5}$$

where $Q_{t+1} = \beta(D_{t+1}/D_t)^{-\alpha}$ is the pricing kernel defined as the intertemporal marginal rate of substitution multiplied by the discount factor.

PROPOSITION 1 (Complete Information): *Assuming that the mean dividend growth rate g_t is subject to breaks, and in the case that a break happens the new mean dividend growth rate is extracted from a univariate density $g_{t+1} \sim G(\cdot)$ with support $[g_d, g_u]$, where $1 + \rho > (1+g_u)^{1-\alpha}$; then the stock and bond prices under complete information, S_t^{CI} and B_t^{CI} respectively, are given by:*

$$S_t^{CI} = \frac{D_t}{1+\rho-(1-\pi)(1+g_t)^{1-\alpha}}\left\{(1-\pi)(1+g_t)^{1-\alpha} + \pi\left(\frac{I_1 + (1-\pi)I_2}{1-\pi I_3}\right)\right\} \tag{6}$$
$$= D_t \Psi(g_t)$$

where

$$I_1 = \int_{g_d}^{g_u} (1+g_{t+1})^{1-\alpha} dG(g_{t+1})$$

$$I_2 = \int_{g_d}^{g_u} \frac{(1+g_{t+1})^{2-2\alpha}}{1+\rho-(1-\pi)(1+g_{t+1})^{1-\alpha}} dG(g_{t+1})$$

$I_3 = \int_{g_d}^{g_u} \frac{(1+g_{t+1})^{1-\alpha}}{1+\rho-(1-\pi)(1+g_{t+1})^{1-\alpha}} dG(g_{t+1})$;

while

$$B_t^{CI} = \frac{1}{(1+\rho)} \left\{ (1-\pi)(1+g_t)^{-\alpha} + \pi \int_{g_d}^{g_u} (1+g_{t+1})^{-\alpha} dG(g_{t+1}) \right\}, \quad (7)$$

in which the one-period risk-free interest rate is defined as $r_t^{CI} = 1/B_t^{CI} - 1$.

Proof: See appendix A

Proposition 1 has multiple repercussions. The ex-dividend stock prices are first order homogeneous in dividends and are affected by breaks in g_t. Consequently, the price-dividend ratio is time-varying and also conditioned to g_t. Similarly, the one-period zero-coupon bond changes over time due to shifts in g_t. The one-period zero-coupon bond price is given by the expected pricing kernel without breaks, $(1+g_t)^{-\alpha}/(1+\rho)$, multiplied by the probability of no breaks plus the expected pricing kernel in the case of breaks, $\int_{g_d}^{g_u}(1+g_t)^{-\alpha} dG(g_t)\,/(1+\rho)$, multiplied by the probability of breaks. Additionally, the current expected forward price of a one-period zero-coupon bond in the very long-term is equal to the expected value of the pricing kernel in the scenario of a break since the probability of having no shifts in the distant future is practically zero (i.e. $\lim_{s\to\infty} E_t[B_s^{CI}] = \int_{g_d}^{g_u}(1+g_t)^{-\alpha} dG(g_t)\,/(1+\rho)$).

Furthermore, pricing European call option contracts is straightforward under complete information. We assume that arbitrage opportunities are not possible, and the agent forms portfolio choices based only on stocks and bonds since markets are complete. In the case of an economy without breaks (i.e. $\pi = 0$), option prices could be estimated by the Black-Scholes model which assumes that the dividend fundamental process is stationary. However, the Black-Scholes model is not valid when breaks in g_t are present. Breaks make dividend yields and interest rates time-varying, thereby introducing nonstationarities into assets. For instance, in an option contract there is a probability that g_t presents a break in the period before its expiration date, which should be taken into account in the option pricing. Therefore, the correct discount

factors are path-dependent. Nevertheless, option contracts can be priced by a change of measure in relation to the state-price density. The following proposition presents an expression for European call option contracts based on this change of measure that will be resolved by numerical methods in the next section.

PROPOSITION 2 (Complete Information): *Under complete information prices of European call option contracts written on the stock with strike price K and time-to-maturity τ are given by:*

$$Call_t^{CI}(K,\tau) = \int_0^{\infty} \max\{S_{t+\tau}^{CI} - K, 0\}\, \tilde{p}_t(S_{t+\tau}^{CI}) dS_{t+\tau}^{CI} \tag{8}$$

where $S_{t+\tau}^{CI} = D_{t+\tau}\Psi(g_{t+\tau})$, $D_{t+\tau} = D_t \exp\left(\sqrt{\tau}\sigma\varepsilon_{t+\tau} - \tau\sigma^2/2\right)\prod_{i=0}^{z}(1+g_{t+h_i})^{h_i}$, $\varepsilon_{t+\tau}$ *is the innovation term of the dividends' geometric random walk in equation* (1) *characterised by a normal density* $\phi(\varepsilon_{t+\tau}|0,\sigma)$ *with mean zero and variance* σ, z *is the number of breaks between* t *and* $t+\tau$ *that is a random variable drawn from a Binomial distribution* $\varphi(z|\tau,\pi)$ *with parameters* τ *and* π, $\{h_i\}_{i=0}^{z}$ *are the time periods between breaks and also random variables drawn from geometric distributions* $\eta(h_i|\pi)$ *in which* $\tau = \sum_{i=0}^{z} h_i$. *In addition,* $\{g_{t+h_i}\}_{i=1}^{z}$ *are drawn from a univariate density* $g_{t+h_{i-1}} \sim G(\cdot)$ *with pdf* $\varrho(\cdot)$ *defined on the support* $[g_d, g_u]$ *where* $g_{t+h_0} = g_t$ *and* $g_{t+\tau} = g_{t+h_z}$, *and finally:*

$$\tilde{p}_t(S_{t+\tau}^{CI}) = \beta^{\tau}\left(\frac{D_{t+\tau}}{D_t}\right)^{-\alpha}\phi(\varepsilon_{t+\tau}|0,\sigma)\varphi(z|\tau,\pi)\eta(h_0|\pi)\left(\eta(h_1|\pi)\varrho\left(g_{t+h_1}\right)\cdot\ldots \cdot\eta(h_z|\pi)\varrho\left(g_{t+h_z}\right)\right).$$

Proof: See appendix A

2.2 *Option Pricing under Breaks and Incomplete Information with Bayesian Learning*

The equations for pricing bond, stock, and option contracts introduced in proposition 1 and proposition 2 were derived assuming that the agent knows the true mean dividend growth rate at each instant. However, these expressions are not valid when there is incomplete information in the economy. Suppose that g_t is unknown and the representative agent uses the information available efficiently to price all assets following a Bayesian updating procedure. The agent observes new independent signals about the mean dividend growth on a daily basis, $\{D_i/D_{i-1}\}_{i=t-n+1}^{t}$, which are random and follow a lognormal distribution where n is the number of periods since the last break (see equation (1)). The representative agent uses her prior beliefs while she recursively learns, incorporating the new information received. Therefore, the expected value of any asset, $\lambda_t(g_t|\pi,\rho,\alpha,\sigma)$, given the agent's prior beliefs $\varrho(g_t)$ can be obtained from the following updating Bayesian rule:

$$\mathrm{E}_{t,n}^{BL}[\lambda_t(g_t)|\mathbf{q}_t] = \frac{\int_{g_d}^{g_u} \lambda_t(g_t) L(g_t|\mathbf{q}_t)_n \varrho(g_t) dg_t}{\int_{g_d}^{g_u} L(g_t|\mathbf{q}_t)_n \varrho(g_t) dg_t} \tag{9}$$

where $L(g_t|\mathbf{q}_t)_n$ is the sample likelihood function, and the vector of signals is represented by $\mathbf{q}_t = [(D_t/D_{t-1}) \dots (D_{t-n+1}/D_{t-n})]$. The intuition behind equation (9) is simple. The agent does not know the new value of g_t after a break; however she knows the distribution followed by g_t (i.e. $\varrho(g_t)$) and the distribution followed by the signals $\mathbf{q}_t$ (i.e. which are lognormally distributed). Given this knowlodge, the agent updates her expectations about g_t and the expectations of all assets that depend of $g_t, \lambda_t(g_t)$, in a recursive process as new signals are observed and learned; which is characterized by the Bayesian procedure presented in equation (9). It is important to mention that after a break the true value of g_t is only partially revealed thanks to the innovation term of the random walk process followed by dividends. Therefore, and additional to the nonstationarities induced in all assets generated by breaks, incomplete information and learning generate extra noise in stock, bond, and option prices.

Furthermore, in equation (9) instead of dealing with a complex sample likelihood function for lognormally distributed data, we take μ_t as the unknown parameter without loss of generality since $1 + g_t = \exp(\mu_t + \sigma^2/2)$. The main advantage of using μ_t as an unknown parameter is that the observable signals, $\{\ln(D_i/D_{i-1})\}_{i=t-n+1}^{t}$, follow a normal density; and thus equation (9) can be written as:

$$\mathrm{E}_{t,n}^{BL}[\lambda_t(\mu_t)|\boldsymbol{\xi}_t] = \frac{\int_{\mu_d}^{\mu_u} \lambda_t(\mu_t) L(\mu_t|\boldsymbol{\xi}_t)_n f(\mu_t) d\mu_t}{\int_{\mu_d}^{\mu_u} L(\mu_t|\boldsymbol{\xi}_t)_n f(\mu_t) d\mu_t} \tag{10}$$

with

$$L(\mu_t|\boldsymbol{\xi}_t)_n = \frac{1}{\sqrt{2\pi\sigma^2/n}} \exp\left[\frac{-\left(\bar{\xi}_t - \mu_t\right)^2}{2\sigma^2/n}\right] \tag{11}$$

in which $\boldsymbol{\xi}_t = [\ln(D_t/D_{t-1}) \ldots \ln(D_{t-n+1}/D_{t-n})]$, and $\bar{\xi}_t = (1/n)\sum_{i=t-n+1}^{t} \xi_i$ is the sample mean. The same properties assumed under full information are still valid. In addition, we assume that the agent knows when a break happens. Although it is possible to extend our setup to include the effects induced by the estimation of breaking dates, the costs of including further complexities make the model less intuitive and results difficult to interpret. Moreover, the assumption of knowledge of breaking dates is not far from reality since there is already a set of studies in which dynamic tests for structural breaks are presented (Chu *et al*. (1996) and Leisch *et al*. (2000)). These studies introduce tests based on a sequential analysis of new observations received progressively for monitoring in real time structural breaks.[7] Consequently, thanks to equation (10) and equation (11) it is possible to present the equations to describe asset prices in the scenario of breaks and incomplete information with learning.

COROLLARY 1 (Bayesian Learning): *Assuming incomplete information and learning, the stock and bond prices are given by:*

[7] Additionally, Lettau and Van Nieuwerburgh (2008) show that the uncertainty generated by the detection of breaking dates of economic fundamentals are not critical in the context of stock returns anomalies. Lettau and Van Nieuwerburgh (2008) show that the main source of uncertainty is caused by the estimation of the magnitude of the new parameter, as it is characterised in our modelling approach.

$$S_t^{BL} = \frac{\int_{\mu_d}^{\mu_u} S_t^{CI} L(\mu_t|\boldsymbol{\xi}_t)_n f(\mu_t) d\mu_t}{\int_{\mu_d}^{\mu_u} L(\mu_t|\boldsymbol{\xi}_t)_n f(\mu_t) d\mu_t} \tag{12}$$

and

$$B_t^{BL} = \frac{\int_{\mu_d}^{\mu_u} B_t^{CI} L(\mu_t|\boldsymbol{\xi}_t)_n f(\mu_t) d\mu_t}{\int_{\mu_d}^{\mu_u} L(\mu_t|\boldsymbol{\xi}_t)_n f(\mu_t) d\mu_t} \tag{13}$$

where S_t^{CI} and B_t^{CI} are the stock and bond price expressions under breaks and complete information defined in proposition 1.

COROLLARY 2 (Bayesian Learning): *Under incomplete information and learning, the prices of European call option contracts with underlying asset S_t, strike price K, and time-to-maturity $\tau = T - t$ are:*

$$Call_t^{BL}(K,\tau) = \frac{\int_{\mu_d}^{\mu_u} \left\{ \int_0^{\infty} \max\{S_{t+\tau}^{CI} - K, 0\} \tilde{p}_t(S_{t+\tau}^{CI}) dS_{t+\tau}^{CI} \right\} L(\mu_{t+\tau}|\boldsymbol{\xi}_{t+\tau})_{n_{t+\tau}} f(\mu_{t+\tau}) d\mu_{t+\tau}}{\int_{\mu_d}^{\mu_u} L(\mu_{t+\tau}|\boldsymbol{\xi}_{t+\tau})_{n_{t+\tau}} f(\mu_{t+\tau}) d\mu_{t+\tau}} \tag{14}$$

where $S_{t+\tau}^{CI} = D_{t+\tau}\Psi(g_{t+\tau})$ with $g_{t+\tau} = \exp(\mu_{t+\tau} + \sigma^2/2) - 1$, while dividends on the expiration date are characterised by $D_{t+\tau} = D_t \exp\left(\sqrt{\tau}\sigma\varepsilon_{t+\tau} - \tau\sigma^2/2\right) \prod_{i=0}^{z}(1 + g_{t+h_i})^{h_i}$ in which $\varepsilon_{t+\tau}$, z, $\{h_i\}_{i=0}^{z}$, $\{g_{t+h_i}\}_{i=1}^{z}$, and $\tilde{p}_t(S_{t+\tau}^{CI})$ were described in Propostion 1. In addition, $n_{t+\tau}$ is the number of signals since the last break.[8]

The simplicity of the Bayesian updating procedure presented in corollary 1 and corollary 2 is extremely useful for understanding the effects of learning on asset prices. Although, it is interesting to analyse firstly two particular cases. Suppose that the probability of a break is very large, $\pi \to 1$; this means that the agent faces breaks every day. In this case, learning is not observable at all since everything changes constantly and 'there is no time to learn'. Additionally, learning should vanish after a while in the case of an economy with no breaks even under incomplete information. In

[8] It is important to observe that $n_{t+\tau} \neq n + \tau$ since there are chances of breaks between t and $t + \tau$; and thus $n_{t+\tau}$ is also a random variable where $n_{t+\tau} \leq n + \tau$.

this case the agent should have sufficient information after a long period to calculate accurate estimates for g_t and asset prices; and thus learning will disappear asymptotically.

Furthermore, corollary 1 and corollary 2 show that after a break, substantial revisions in the agent's expectations are present which strongly affect asset prices. Immediately after breaks, the agent does not have enough historical information to obtain reliable estimates. Therefore, the agent experiences an initial intense period of learning that generates important changes in her beliefs, which induces premiums in the valuation process of all assets and particularly in option prices and their implied volatilities. However, these large adjustments in the beliefs are reduced over time as more information is received and learned. This updating process of the agent's beliefs, which is caused by the recursive information acquisition, should induce predictable dynamics on option prices and implied volatilities such as serial correlations among other dynamic effects, which we will test in the following section.

3 Simulations and Results

3.1 Simulations

The main aim of our research is the analysis of the effects of the learning process on the dynamics and qualitative behaviours of option pricing using different assumptions about agents' expectations. Following the same arguments as in Timmermann (1993, 1996), who evaluates how the learning process affects univariate stock returns by simulation methods, we use a simulation approach to analyse the learning effects on option securities. Timmermann (1993, 1996) argues that learning influences the investors' pricing in a highly nonlinear way and hence a simulation analysis is necessary to understand the wide scope of outcomes that learning induces in assets. In addition, Kleidon (1986) shows that the use of standard tests to evaluate an equilibrium model using a single economy represented by market data could lead to inaccurate analyses. Kleidon (1986) points out that asset prices in equilibrium are calculated based on agents' expectations about future events across multiple and

different economies. Therefore, the use of a specific realization given by market prices could induce wrong conclusions. Instead, Kleidon (1986) also proposes the use of multiple realizations by simulation techniques. Moreover, the use of simulation allows us to modify parameters setups and thus to observe the impacts of learning on multiple environments.

As a first step in the simulations, we reproduce the CBOE rules to create option contract series in terms of strike price intervals, expiration dates, and listing and delisting policies. In previous studies, simulated option data have been performed assuming constant moneyness and time-to-maturity for a specific option contract (e.g. exactly 30-days option contracts with the moneyness equal to one).[9,10] However, on the one hand, the moneyness ratio changes constantly because strike prices are fixed by option exchanges while stock prices vary over time. On the other hand, the time-to-maturity decreases gradually since expiration dates are also fixed. Therefore, the assumption of regular and invariable features of option contracts is not comparable with option market data. Instead, we generate option data following the Chicago Board Option Exchange (CBOE) normative to obtain a picture closer to reality than existing studies. First, we use the same trading dates that took place in the 12 years between 1996 and 2007, and thus accounting for holidays and unexpected events in which the market was closed. Second, we fix expiration dates for option contracts in the same way as the CBOE. Therefore, the expiration dates are in the three subsequent close months followed by three further long-term months from the March quarterly cycle (i.e. March, June, September, and December). In addition, expiration dates are on the Saturday after the third Friday of each expiration month. In relation to strike price intervals, they are around the underlying asset price where option contracts with expiration dates in the three near-term months have 5-point intervals; while option contracts for long-term months have 25-point intervals.

We calculate implied volatilities by numerically inverting the Black-Scholes (1973) model (henceforth, the BS model) which is consistent with academic studies and investors practices. It is evident that the Black-Scholes (1973) assumptions are not

[9] See, e.g., Duan and Simonato (2001) and Yan (2011).
[10] We define the moneyness as $Mon = K/S$ where K and S are strike and stock prices, respectively.

followed by our learning model. However, researchers and practitioners also calculate the implied volatilities using the BS model even thought they know that the Black-Scholes (1973) assumptions are violated in the market data. Moreover, the well known predictability patterns in both implied volatilities and the shape features of *IVS*, which we want to explain through our learning model, have been observed using implied volatilities calculated with the BS model (e.g. Harvey and Whaley (1992), Gonçalves and Guidolin (2006), Konstantinidi *et al*. (2008), and Chalamandaris and Tsekrekos (2010)). Consequently, we also calculate the implied volatilities using the BS model following the market practices; and thus to observe whether the agents learning process descried in our model can replicate the puzzling dynamic behaviour of the implied volatilities and the *IVS*.

We assume the following plausible parameter values to be used in the simulations. The rate of impatience, ρ, is set at 8.9% and 9.6% (annual basis). We also assume that when ρ=8.9% (ρ=9.6%) the new mean dividend growth rate after breaks is extracted from a uniform distribution defined between $g_u = 8.8\%$ ($g_u = 9.5\%$) and $g_d = -1.5\%$ ($g_d = -5.0\%$); and thus $1 + \rho > (1 + g_u)^{1-\alpha}$.[11] The dividend process volatility, σ, is also set at two values, 5% and 30% (annual basis); and we calculate asset prices using multiple levels for the coefficient of relative risk aversion. Moreover, we use the test introduced by Chu *et al.* (1996) to calculate the probability of breaks, π, on the mean dividend growth. Chu *et al.* (1996) present a dynamic test for structural breaks where market participants can identify contemporaneously a break on a given date due to the real-time features of their algorithm. We perform this test to calculate π using daily dividend time series from the S&P 500 index between 1996 and 2007 which are deseasonalized and adjusted by the consumer price index to obtain real dividends. We find eight breaks in the 3012 days of the 12 years analyzed; and thus we set π at 0.67 (annual basis). In appendix C, we describe the model introduced by Chu *et al.* (1996) and the breaks detected.

[11] Therefore, and given that the new mean dividend growth rate after breaks is extracted from a uniform distribution with probability density function $f(g_t) = 1/(g_u - g_d)$, in corollary 1 and corollary 2 the dividend drift has as probability density function: $f(\mu_t) = \exp(\mu_t + \sigma^2/2)/(g_u - g_d)$, where $\mu_d = \ln(1 + g_d) - \sigma^2/2$ and $\mu_u = \ln(1 + g_u) - \sigma^2/2$.

As mentioned previously we simulate multiple scenarios depending on three assumptions about the agent's expectations: i) an economy without breaks; ii) an economy with breaks and complete information; and iii) and an economy with breaks and incomplete information incorporating learning. First, in the case without breaks (i.e. g_t constant) we calculate stock and bond prices assuming that $\pi = 0$ using equation (6) and equation (7), respectively. In this case, European call option contract prices are obtained by the Black-Scholes (BS) model in which the dividend yield is $\delta^{BS} = (1 + \rho - (1 + g_t)^{1-\alpha})/(1 + g_t)^{1-\alpha}$. Second, in the scenario of an economy with breaks and complete information, stock and bond prices are calculated through equation (6) and equation (7) assuming that $\pi = 0.67$. In addition, European call option prices are calculated using equation (8) where the main integral is resolved by Monte Carlo simulations, which are based on 7,000 paths following the stochastic process described in proposition 2. Third, in the case of breaks and incomplete information with learning, the values for stock and bond prices are obtained using equation (12) and equation (13) with $\pi = 0.67$; while option prices are obtained with equation (14) and also using Monte Carlo simulations with 7,000 paths.[12]

In each assumption about the agent's expectations and in each combination of parameters we generate 1,000 simulations. In each simulation we produce 12 years of daily dividends (3018 days) which are the observable signals received by agents to learn about g_t and thus to price assets. The simulations are generated by the two nested stochastic processes described in equation (1). This means we simulate time series of 12 years of daily dividends using the dividend's geometric random walk process. However, we induce breaks in g_t in each simulation (and hence breaks in μ_t) in which periods between breaks follow a geometric process with parameter π. For instance, in the case in which a break occurs at time $t + m$, we obtain a new value for g_{t+m} drawn from a uniform distribution $g_{t+m} \sim U(\cdot)$ defined on the support $[g_d, g_u]$, and we keep this value constant until the next break.

[12] In addition, in the Monte Carlo simulations we simultaneously estimate the expected dividend yield and expected zero curves for the 'life' of each option contract with the objective of calculating later implied volatilities.

Furthermore, although we price stock and bond securities in the simulations daily, we calculate option prices for all option contracts only on Wednesday of each week.[13] This is due to the high computational resources required by the Monte Carlo methods used to price the option securities through equation (8) and equation (14). Monte Carlo methods are intensely used to calculate option prices in our simulation analysis since they are required in four combined dimensionalities: i) in each of the 1,000 simulations; ii) in each simulation over 12 years; iii) in multiple option contracts across moneyness and maturity in each simulation of 12 years; and iv) in several sets of 1,000 simulations using diverse parameter setups and in different agent's expectations.[14]

3.2 Results

The existence of breaks in the mean dividend growth rate and learning introduce nonstationarities into stock, bond, and option prices. For instance, Figure 1 presents outcomes of one of the simulations under three scenarios: i) no breaks; ii) breaks and complete information; and iii) breaks and incomplete information with learning. Figure 1 reports evolutions of the mean dividend growth rate (upper window), stock prices (middle window), and implied volatilities of approximately short-term at-the-money call option contracts (lower window).[15,16] In addition, it is important to mention in relation to Figure 1 that in the second and third scenarios, where breaks are present, dividends are exactly the same and hence the observable signals received

[13] The selection of Wednesdays is to minimize the incidence of the number of holidays in our analysis since we use in the simulations authentic U.S. trading dates that took place between 1996 and 2007.
[14] Even after obtaining option prices only on Wednesdays, the simulation analysis presented in this study was only possible thanks to the use of 20 processors running for 76 days in a computing grid.
[15] A short-term at-the-money option contract is assumed to be a contract with 30-days (calendar days) to the expiration and $K/S = 1$. Consequently, implied volatilities are calculated by simple linear interpolation using the four contracts around the 30-days time-to-maturity and with closest strike prices to the underlying stock prices.
[16] In figure 1 lower window we present implied volatilities instead of option prices because implied volatilities can be interpreted and analysed more easily than their respective option prices. The use of prices of different option contracts is not recommendable for comparative analyses due to the fact that option prices differ in 'level' depending on the option contract characteristics. Instead, implied volatilities can be used to compare all option contracts because they 'should' not suffer from 'level' issues.

by the economic agent about g_t are equal. However, the distinction between the time series in the last two scenarios reflects how learning affects the agent's estimates.

[Insert Figure 1 here]

Figure 1 upper window reports how the learning process affects firstly the agent's estimations about g_t over time. Estimates of g_t follow progressive adjustments toward the true values after each break. On the one hand, as we explained in the prior section, the observable signals received by investors and represented by dividends are noisy thanks to the innovation term of the geometric random walk process. Consequently, the agent needs time to learn and thus to obtain accurate values for the unknown variables. On the other hand, a new break appears when learning has improved the accuracy of the agent's estimations and hence cognitive mechanisms are intense once again. Figure 1 middle window reports that stock prices, in this particular simulation, in the scenarios with breaks (the last two cases) are substantially lower than the prices with no breaks. This result is due to lower g_t values in the scenarios with breaks than in the stationary scenario through the whole simulated period (see Figure 1 upper window). In addition, Figure 1 lower window shows that intense revision of the agent's expectations about the new value of g_t induces an increase in the implied volatilities, especially immediately after breaks when there is an intensive learning process. Moreover, this lower window shows symptoms of serial correlation and volatility clustering on option implied volatilities, which will be tested statistically in posterior analyses. Therefore, Figure 1 lower window presents the first set of evidence to support our contention that the agent's learning process affects the option pricing inducing dynamic premiums.

The nonstationarities generated by learning have an effect on the entire economy. For instance, Table I and Table II report summary statistics of the simulations for the observable dividends and the estimates for the mean dividend growth rate, the interest rate, the stock price, and the short-term at-the-money option contract price and its implied volatility. Table I and Table II present results of the simulations generated by two subsets of parameter combinations and also under three scenarios: no breaks; breaks and complete information; and breaks and incomplete information

with learning. In Table I and Table II, we set the coefficient of relative risk aversion, α, at 0.2, while the rest of the parameters have some differences. We report additional summary statistics in appendix D Table DI to Table DIV, in which we set α at 0.5 and 5.0 using the same combination of parameters and scenarios as in Table I and Table II.

[Insert Table I here]

[Insert Table II here]

Table I and Table II show that dividends are exactly the same for the scenarios with breaks (i.e. the case with complete information, and the case with incomplete information and learning). Additionally, it is particularly interesting to observe in Table I and Table II that the standard deviation of g_t is higher in the scenario with breaks and complete information than in the case of breaks and learning, which is easily understood observing the upper window in Figure 1. The upper window in Figure 1 shows big changes in g_t on breaking dates in the case of breaks and complete information, because shifts in g_t are immediately recognized by the agent. In contrast, in initial periods after a break under an economy with Bayesian learning the agent recursively incorporates new information giving more weight to her prior beliefs, and thus producing gradual movements and adjustments.

A comparison of the first two scenarios in Table I and Table II, which describe complete information with and without breaks, shows that breaks by themselves induce an increase in implied volatilities. However, this effect is smaller than the impact of the information incompleteness and learning. For instance, Table I (Table II) shows that implied volatilities increase from 5.75% (31.63%) in the scenario under breaks and full information to 19.24% (43.28%) in the case under breaks and incomplete information with learning. In addition, Table I and Table II report that learning also induces skewness and kurtosis in option prices and implied volatilities.

The learning effects are also deeply influenced by the agent's attitudes toward risks. Figure 2 shows a sensitivity analysis using diverse relative risk-aversion levels to observe *IVS* shape features in an economy under breaks and incomplete information

with learning. Figure 2 reports the average behaviour of the implied volatilities of multiple option contracts *one month* after a break in g_t. In Figure 2, the average values of the implied volatilities are presented across both the moneyness dimension using short-term option contracts (upper windows) and the maturity dimension by the use of at-the-money option contracts (lower windows).

[Insert Figure 2 here]

Figure 2 upper windows presents that learning induces the typical reverse skew shapes in implied volatilities through the moneyness. Options contract prices are calculated using nonlinear functions, and thus the nonlinear features of the option pricing induce asymmetric effects of learning on different option contracts; in this case, heterogeneous impacts across strike prices. In addition, Figure 2 upper windows report a negative relationship between α and implied volatility levels when $\alpha < 1$, while the relationship is positive when $\alpha > 1$. The intuition behind these results is simple. Learning has the lowest impact on stock and option prices when $\alpha = 1$ since the parts of the valuation formulas that includes the unknown parameter g_t disappear (see both equation (6) and equation (14)).[17] Moreover, Figure 2 upper windows report that when $\alpha < 1$, slopes and curvatures on the moneyness dimension increase with α; while if $\alpha > 1$, slopes and curvatures of the implied volatility reverse skew decrease as α grows. These results are explained by a combination of two main effects: nonlinear asymmetric learning consequences, and a heterogeneous vanishing course of action of the learning impacts on option pricing when α takes values close to one. As we explained earlier, the asymmetric learning effects induce reverse skews on implied volatilities across moneyness, in which the strongest effects are observed on in-the-money option contracts. Furthermore, learning outcomes start to vanish as the relative risk aversion is close to one. However, as α gradually moves closer and closer to one, the learning effects do not disappear proportionately for all the option contracts. The learning impacts vanish slowly for in-the-money option contracts in relation to out-of-the-money option contracts, thus inducing negative steeper slopes and higher curvatures when $\alpha \to 1$ than in other cases. In the case when $\alpha = 1$, the

[17] In equation (6) and equation (14) $\lim_{\alpha \to 1}(1 + g_t)^{1-\alpha} = 1$.

implied volatility reverse skew collapses to a flat curve where implied volatilities under breaks and complete information are equal to the case under breaks and learning.

Figure 2 lower windows show that learning also induces reverse skews in the implied volatility term-structure, where implied volatility levels decrease as the time-to-maturity increases in option contracts. Immediately after a break there are intense revisions about the new value of g_t; however, the Bayesian agent expects that she will learn progressively in the future because she will receive further information in the following periods. These expectations of future learning induce low implied volatilities for long-term option contracts in relation to short-term option contracts. Furthermore, Figure 2 lower windows report that implied volatility levels are lowest when the relative risk aversion is close to one. This is explained with reference to the same arguments used in Figure 2 upper windows where it is shown that the learning effects on stock and option prices are minimal when $\alpha = 1$. Therefore, Figure 2 presents evidence to support the claim that our Bayesian learning model is consistent and explains the large empirical literature that reports implied volatilities variations across moneyness and time-to-maturity (e.g. Rubinstein (1985), Dumas et al. (1998), and Das and Sundaram (1999)).

Figure 3 reports a similar sensitivity analysis in relation to α as Figure 2; however, we present the average behaviour of implied volatilities *one year* later from a break in g_t. The comparative analysis of Figure 2 and Figure 3 allows us to observe the learning effects over time on the *IVS* using diverse relative risk aversion levels. Figure 2 and Figure 3 show that implied volatilities decrease as more information is received since large changes in the agent's beliefs due to an initial intense revision regarding the new level of g_t are reduced thanks to the learning process. Nevertheless, the learning effects do not disappear completely, even after a year. In addition, Figure 3 right-hand upper window shows that implied volatilities on the moneyness dimension describe convex functions for α values close to one when $\alpha > 1$; however, as α increases, the implied volatilities describe concave curves. The main reason for those concave shapes is that when $\alpha > 1$, representative agent endowment economic models in general have a counter-intuitive feature in which stock prices are lower when g_t

increases (see Abel (1988) and Cecchetti *et al.* (1990)); that induces, among other effects, these concave implied volatilities curves on the moneyness dimensions.[18]

[Insert Figure 3 here]

Additionally, we analyse statistically the effects of learning on both the implied volatility dynamics and the *IVS* movements. Table III shows the dynamic features of the implied volatility and the *IVS* shape characteristics under an economy that presents breaks and incomplete information with learning. The results presented in Table III are obtained from simulations using two different parameter setups; however in appendix D, Table DV and Table DVI, we report further parameter combinations as robustness check. We define $Slope_{Mon}$ ($Slope_{Mat}$) as the average of numerical first derivatives using all pairs of moneyness-consecutive 30-days (maturity-consecutive at-the-money) implied volatilities. In addition, $Curv_{Mon}$ ($Curve_{Mat}$) is the average of numerical second derivatives using all trios of moneyness-consecutive 30-days (maturity-consecutive at-the-money) implied volatilities.[19,20] Table III shows that, on average, learning induces negative slopes and convex curves on both moneyness and maturity dimensions. Learning generates kurtosis, serial correlation, and volatility clustering on the implied volatility and slopes and curvatures of the *IVS*. The implied volatility and all shape features of the *IVS* present significant serial correlation effects on more than 50% of the simulations using the first order Ljung-Box test statistic. Furthermore, the implied volatility and slopes and curvatures of the *IVS* under learning report on average significant volatility

[18] Despite this counter-intuitive feature of equilibrium models when $\alpha > 1$, we include them in the analyses to be in line with the large literature in which α values larger than one have been estimated or used to explain diverse issues on asset prices and returns.

[19] The numerical first derivative is $f'(x_1) = (f(x_1) - f(x_0))/(x_1 - x_0)$, while the numerical second derivative is $f''(x_1) = (f(x_2) - 2f(x_1) + f(x_0))/(0.5(x_2 - x_0))^2$.

[20] An alternative way to characterize the *IVS* shape characteristics is through deterministic *IVS* models, which describe the implied volatilities as a function of factors related to strike prices and time-to-maturities (see Dumas et al. (1998)). Moreover, these polynomial functional forms have been successfully used for predictability purposes (e.g. Gonçalves and Guidolin (2006)). However, deterministic *IVS* models impose cross-sectional relationships among the different factors that could add noise to the analysis of our theoretical equilibrium model. Instead, we prefer the simplicity of numerical derivatives which are calculated independently in each dimension (i.e. moneyness and maturity dimensions). However, as a robustness check we report the fitting properties of the implied volatilities obtained by our modelling approach in relation to a deterministic *IVS* model type as per Dumas et al. (1998) in appendix E.

clustering dynamics using the LM test for ARCH effects suggested by Engle (1982) with one and three lags. However, ARCH effects are lower for the slope and curvature on the moneyness dimension, although significant on more than 20% of the simulations. Nevertheless, we will show in the following analysis that predictability patterns also decrease for slopes and curvatures on the moneyness dimension of the *IVS*s in the U.S. option market in a similar way to the results reported by our Bayesian learning model.

[Insert Table III here]

The results presented in Table III are consistent with the empirical evidence reported in the literature about the predictable dynamics in the *IVS* (e.g. Harvey and Whaley (1992), Gonçalves and Guidolin (2006), Fengler *et al.* (2007), and Konstantinidi *et al.* (2008)). In this context, we report in Table IV an analysis equivalent to Table III but using U.S. option market data between 1997 and 2007. Table IV Panel A (Panel B) reports the predictability patterns of the *IVS* using S&P 500 index options (150 equity options in which the underlying stocks pay dividends).[21] The option data used in this table is described in appendix B. Predictability patterns in the *IVS* which are presented in Table III and Table IV (last three columns) show the similarities of the implied volatilities dynamics between the results obtained by our Bayesian learning model and the behaviour observed in option market data. Table IV presents serial correlation and ARCH effects on the implied volatility and slopes and curvatures of the *IVS* in traded option contracts, which are comparable to results obtained by our simulations, even though we use only plausible parameter values in the equilibrium model. Table IV reports that the predictable dynamics decline for slope and curvature on the moneyness dimension analogously to results of the simulations presented in Table III. Moreover, the average implied volatility shape characteristics in Table IV (column 2 to column 4) of S&P 500 index options and equity options are similar to the values reported in Table III. Slopes and curvatures of the *IVS* presented in Table III

[21] Although equity options are American-style, there is empirical evidence showing that they follow similar multivariate dynamics to European option contracts such as S&P 500 index options (see, e.g., Dennis and Mayhew (2002), Goyal and Saretto (2009), and Bernales and Guidolin (2011)). In addition, possible differences have low relative importance in comparison to the enormous benefits of observing multiple dynamic behaviours by the use of 150 different equity options.

and Table IV have the same sign and equivalent magnitudes. The only difference is observed in the mean of the slope and curvature on the maturity dimension for S&P 500 index options. However, we will show in following econometric tests that when there are high levels of uncertainty (where strong learning activities should be present) in S&P 500 index options, maturity slopes tend to be negatively sloped which is consistent with our learning arguments.

[Insert Table IV here]

The agent's learning process also affects how the implied volatility and the *IVS* shape characteristics are related to each other cross-sectional. Table V (Table VI) shows the cross-sectional relationships of the implied volatility and the *IVS* features in an economy under breaks and learning using the simulations generated by the learning model (using option market data). These tables present correlation analyses among the implied volatility and slopes and curvatures of the *IVS*. Table V reports correlations in the simulations using two sets of parameters; nevertheless in appendix D, Table DVII and Table DVIII report further correlation analyses using multiple parameter values. Table V and Table VI reveal that our learning model also explains cross-sectional behaviours of the implied volatility and the *IVS* shape properties observed in option markets. For instance, Table V shows that implied volatility levels obtained from our learning model are negatively related to implied volatility slopes on both maturity and moneyness dimensions in a similar way to S&P 500 index options and equity options in Table VI. Elevated implied volatilities in our modelling approach are associated with an intensive learning process; and thus strong cognitive effects have important but different impacts on option contracts across moneyness and time-to-maturity, inducing steeper negative slopes in the *IVS* shape.

[Insert Table V here]

[Insert Table VI here]

Finally, it is important to mention that option markets have been widely used to capture forward-looking information since they reflect agents' expectations about

future scenarios, in which forecasting horizons match the expiration dates of options contracts. The information captured from option prices has been used by investors in all markets and in a broad spectrum of financial issues including risk management, asset allocation, and trading strategies.[22] However, through our model and its analysis and results we show that option markets do not have only forward-looking features; they also have backward-looking characteristics since option investors learn recursively as new information arrives. Participants in option markets face a sequential process of information acquisition in which economic signals are received and processed with reference to the historical information and prior beliefs. Therefore, the forward-looking information obtained from option markets is generated by a backward-looking learning process.

4 Conclusions

The fact that option prices and implied volatilities are predictable has been identified by academics and exploited by practitioners. Nevertheless, there is a gap in the literature regarding possible explanations for such puzzling predictability patterns. We contribute to the body of knowledge by showing evidence to support the hypothesis that the investors' learning plays an important role in explaining diverse dynamics in the option prices. We present an equilibrium model where the unknown fundamental dividend growth rate is subject to breaks. A representative agent receives independent but noisy signals about the unknown fundamental value daily; which are used efficiently following a Bayesian learning process. We show that learning explains several anomalies in relation to predictability patterns of option prices observable in the market. We find that the learning process makes the agent's beliefs time-varying which induces dynamic premiums in option prices and implied volatilities. Moreover, our modelling approach shows that learning generates different dynamics on option contracts depending of their moneynesses and time-to-maturities,

[22] For instance, option prices have been used for forecasting purposes in asset returns (e.g., Xing *et al.* (2010), Cremers and Weinbaum (2010), and Bakshi *et al.* (2011)), realized volatilities (e.g. Christensen and Prabhala (1998), and Busch *et al.* (2011)), risk premiums (e.g. Duan and Zhang (2010)), betas (e.g. Siegel (1995), and Chang *et al.* (2009)), correlation coefficients (e.g. Driessen *et al.* (2009)), and to perform asset allocations (e.g. Kostakis *et al.* (2011)).

which induce movements in the *IVS* shape. Furthermore, learning mechanisms make the dynamics of option prices predictable. Similarly to the predictability features observable in option market data, the results obtained in the simulation analysis report serial correlations and volatility clustering in the implied volatility and slopes and curvatures of the *IVS*. Finally, the model presented in our study is simple and intuitive; however other interesting issues remain to be addressed. The study of possible learning effects on trading decisions in portfolios including option contracts is beyond the scope of this paper; while the study of the impact of learning on option returns is left for future research.

Appendix A

Proof of Proposition 1: Assuming that the expression that describes S_t^{CI} can be written as $S_t^{CI} = D_t\Psi(g_t)$ for some function $\Psi_t^{CI}(\cdot)$, we define a 'break indicator', s_t, in relation to the mean dividend growth rate. In the case in which there is no break in g_{t+1} $s_{t+1} = s_t$; and if $s_{t+1} = s_t + 1$, a break has taken place at $t+1$. Additionally, $\Pr(s_{t+1} = s_t) = (1-\pi)$ is the probability of no break, and the probability of a break out of the state prevailing at time t is $\Pr(s_{t+1} = s_t + 1) = \pi$. Therefore, from equation (4):

$$
\begin{aligned}
&(1+\rho)\Psi(g_t)D_t \\
&= \sum_{i=0}^{1} E_t\left[(\Psi_t^{CI}(g_t)D_{t+1} + D_{t+1})\left(\frac{D_{t+1}}{D_t}\right)^{-\alpha} | s_{t+1} = s_t + \mathrm{i}\right]\Pr(s_{t+1} = s_t + i) \\
&= (1-\pi)\, D_t \int_{-\infty}^{\infty}\left(1 + \Psi_t^{CI}(g_t)\right)(1+g_t)^{1-\alpha}\exp\left((1-\alpha)\left(\sigma\varepsilon_{t+1} - \frac{\sigma^2}{2}\right)\right) \\
&\cdot \phi(\varepsilon_{t+1}|\sigma^2)d\varepsilon_{t+1} + (1-e^{-\pi})D_t \int_{g_d}^{g_u}\int_{-\infty}^{\infty}(1+\Psi_t^{CI}(g_{t+1}))\,(1+g_{t+1})^{1-\alpha} \\
&\cdot \exp\left((1-\alpha)\left(\sigma\varepsilon_{t+1} - \frac{\sigma^2}{2}\right)\right)\phi(\varepsilon_{t+1}|\sigma^2)\, d\varepsilon_{t+1}dG(g_{t+1})
\end{aligned}
\tag{A1}
$$

where $G(\cdot)$ is the cumulative distribution function of g_{t+1} defined on $[g_d, g_u]$, ε_{t+1} is the innovation term of the dividends' geometric random walk, and $\phi(\cdot\,|\sigma)$ is a normal density function with mean zero and variance σ. Therefore, given that ε_{t+1} and g_{t+1} are independent, we can rewrite equation (A1) as:

$$\begin{aligned}(1+\rho)\Psi(g_t)D_t &= (1-\pi)D_t(1+g_t)^{1-\alpha}(1+\Psi_t^{CI}(g_t)) \\ &+ \pi D_t \int_{g_d}^{g_u}(1+g_{t+1})^{1-\alpha}dG(g_{t+1}) \; + \pi D_t \int_{g_d}^{g_u}\Psi_t^{CI}(g_{t+1})(1+g_{t+1})^{1-\alpha}dG(g_{t+1})\end{aligned} \tag{A2}$$

or equivalently,

$$\begin{aligned}D_t\Psi(g_t) &= (1-\pi)\frac{D_t}{1+\rho-(1-\pi)(1+g_t)^{1-\alpha}}(1+g_t)^{1-\alpha} \\ &+ \pi\frac{D_t}{1+\rho-(1-\pi)(1+g_t)^{1-\alpha}}\int_{g_d}^{g_u}(1+g_{t+1})^{1-\alpha}dG(g_{t+1}) \\ &+ \pi\frac{D_t}{1+\rho-(1-\pi)(1+g_t)^{1-\alpha}}\int_{g_d}^{g_u}\Psi_t^{CI}(g_t)(1+g_{t+1})^{1-\alpha}dG(g_{t+1}).\end{aligned} \tag{A3}$$

Subsequently and assuming that $G(\cdot)$ does not vary over time in equation (A3), we multiply both sides by $(1+g_{t+1})^{1-\alpha}dG(g_{t+1})/D_t$ and integrate over $[g_d, g_u]$:

$$\begin{aligned}\int_{g_d}^{g_u}\Psi(g_t)(1+g_t)^{1-\alpha}dG(g_t) &= \int_{g_d}^{g_u}(1-\pi)\frac{(1+g_t)^{2-2\alpha}}{1+\rho-(1-\pi)(1+g_t)^{1-\alpha}}dG(g_t) \\ &+ \int_{g_d}^{g_u}\pi\frac{(1+g_{t+1})^{1-\alpha}\int_{g_d}^{g_u}(1+g_{t+1})^{1-\alpha}dG(g_{t+1})}{1+\rho-(1-\pi)(1+g_{t+1})^{1-\alpha}}dG(g_{t+1}) \\ &+ \int_{g_d}^{g_u}\pi\frac{(1+g_{t+1})^{1-\alpha}}{1+\rho-(1-\pi)(1+g_{t+1})^{1-\alpha}}dG(g_{t+1}) \\ &\cdot \int_{g_d}^{g_u}\Psi(g_{t+1})(1+g_{t+1})^{1-\alpha}dG(g_{t+1}).\end{aligned} \tag{A4}$$

The term on the left side is equal to the second part of last term on the right side, and consequently:

$$\begin{aligned}
&\int_{g_d}^{g_u} \Psi(g_{t+1})(1+g_{t+1})^{1-\alpha} dG(g_{t+1}) \\
&= \left(\int_{g_d}^{g_u} (1-\pi) \frac{(1+g_{t+1})^{2-2\alpha}}{1+\rho-(1-\pi)(1+g_{t+1})^{1-\alpha}} dG(g_{t+1}) \right. \\
&\left. + \int_{g_d}^{g_u} \pi \frac{(1+g_{t+1})^{1-\alpha} \int_{g_d}^{g_u} (1+g_{t+1})^{1-\alpha} dG(g_{t+1})}{1+\rho-(1-\pi)(1+g_{t+1})^{1-\alpha}} dG(g_{t+1}) \right) \\
&/ \left(1 - \int_{g_d}^{g_u} \pi \frac{(1+g_{t+1})^{1-\alpha}}{1+\rho-(1-\pi)(1+g_{t+1})^{1-\alpha}} dG(g_{t+1}) \right).
\end{aligned} \tag{A5}$$

Finally, inserting equation (A5) into equation (A3):

$$\begin{aligned}
S_t^{CI} &= \frac{D_t}{1+\rho-(1-\pi)(1+g_t)^{1-\alpha}} \left\{ (1-\pi)(1+g_t)^{1-\alpha} \right. \\
&+ \pi \int_{g_d}^{g_u} (1+g_{t+1})^{1-\alpha} dG(g_{t+1}) \\
&+ \pi \left(\int_{g_d}^{g_u} (1-\pi) \frac{(1+g_{t+1})^{2-2\alpha}}{1+\rho-(1-\pi)(1+g_{t+1})^{1-\alpha}} dG(g_{t+1}) \right. \\
&\left. + \int_{g_d}^{g_u} \pi \frac{(1+g_{t+1})^{1-\alpha} \int_{g_d}^{g_u} (1+g_{t+1})^{1-\alpha} dG(g_{t+1})}{1+\rho-(1-\pi)(1+g_{t+1})^{1-\alpha}} dG(g_{t+1}) \right) \\
&\left. / \left(1 - \int_{g_d}^{g_u} \pi \frac{(1+g_{t+1})^{1-\alpha}}{1+\rho-(1-\pi)(1+g_{t+1})^{1-\alpha}} dG(g_{t+1}) \right) \right\}.
\end{aligned} \tag{A6}$$

The integrals in equation (A6), which are constant over time, can be labelled as:

$$I_1 = \int_{g_d}^{g_u} (1+g_{t+1})^{1-\alpha} dG(g_{t+1}) \tag{A7}$$

$$I_2 = \int_{g_d}^{g_u} \frac{(1+g_{t+1})^{2-2\alpha}}{1+\rho-(1-\pi)(1+g_{t+1})^{1-\alpha}}\, dG(g_{t+1}) \tag{A8}$$

$$I_3 = \int_{g_d}^{g_u} \frac{(1+g_{t+1})^{1-\alpha}}{1+\rho-(1-\pi)(1+g_{t+1})^{1-\alpha}}\, dG(g_{t+1}) \tag{A9}$$

and thus,

$$\begin{aligned} S_t^{CI} &= \frac{D_t}{1+\rho-(1-\pi)(1+g_t)^{1-\alpha}} \left\{(1-\pi)(1+g_t)^{1-\alpha} + \pi I_1 \right. \\ &\left. + \pi\left(\frac{(1-\pi)I_2 + \pi I_1 I_3}{1-\pi I_3}\right)\right\} \\ &= \frac{D_t}{1+\rho-(1-\pi)(1+g_t)^{1-\alpha}} \left\{(1-\pi)(1+g_t)^{1-\alpha} + \pi\left(\frac{I_1+(1-\pi)I_2}{1-\pi I_3}\right)\right\}. \end{aligned} \tag{A10}$$

Therefore, equation (A10) shows that $S_t^{CI} = D_t \Psi_t^{CI}(g_t)$, as we state in equation (A1). □

In the case of the bond, we use the second Euler equation (5) to obtain its price:

$$\begin{aligned} B_t^{CI} &= \frac{1}{(1+\rho)} \sum_{i=0}^{1} \mathrm{E}_t\left[\left(\frac{D_{t+1}}{D_t}\right)^{-\alpha} | s_{t+1} = s_t + \mathrm{i}\right] \Pr(s_{t+1} = s_t + i) \\ &= \frac{1}{(1+\rho)} \left\{(1-\pi) \int_{-\infty}^{\infty} (1+g_t)^{-\alpha} \exp\left(-\alpha\left(\sigma\varepsilon_{t+1} - \frac{\sigma^2}{2}\right)\right) \phi(\varepsilon_{t+1}|\sigma^2) d\varepsilon_{t+1} + \pi \right. \\ &\left. \cdot \int_{g_d}^{g_u} \int_{-\infty}^{\infty} (1+g_{t+1})^{-\alpha} \exp\left(-\alpha\left(\sigma\varepsilon_{t+1} - \frac{\sigma^2}{2}\right)\right) \phi(\varepsilon_{t+1}|\sigma^2)\, d\varepsilon_{t+1} dG(g_{t+1}) \right\} \\ &= \frac{1}{(1+\rho)} \left\{(1-\pi)(1+g_t)^{-\alpha} + \pi \int_{g_d}^{g_u} (1+g_{t+1})^{-\alpha} dG(g_{t+1}) \right\}. \end{aligned} \tag{A11}$$

The last equality is obtained assuming that $G(\cdot)$ does not vary over time and by the independence of ε_{t+1} and g_{t+1}. □

Proof of Proposition 2: This equation can be obtained from no-arbitrage arguments with respect to a contingent claim with value given by $\max\{S_{t+\tau}^{CI} - K\}$ where the mean dividend growth rate is subject to breaks. Therefore, it is necessary to prove that the probabilities that describe the state price density are risk-neutralized. Following Huang and Litzenberger (1988, p. 229), we take the Euler equation (4) which is divided by the one-period zero-coupon with unit price to the expiration:

$$\frac{(1+\rho)S_{t+k}^{CI}}{(1-\pi)(1+g_{t+k})^{-\alpha} + \pi\int_{g_d}^{g_u}(1+g_{t+k})^{-\alpha}dG(g_{t+k})} = \mathrm{E}_{t+k}\left[\beta\left(\frac{D_{t+\mathrm{k}+1}}{D_{t+k}}\right)^{-\alpha} \cdot (S_{t+k+1}^{CI} + D_{t+k+1})\frac{(1+\rho)}{(1-\pi)(1+g_{t+k})^{-\alpha} + \pi\int_{g_d}^{g_u}(1+g_{t+k})^{-\alpha}dG(g_{t+k})}\right]. \quad \text{(A12)}$$

We assume that the forward price and the forward cumulative dividend process are:

$$S_{t+k}^{CI^*} = \frac{(1+\rho)S_{t+k}^{CI}}{(1-\pi)(1+g_{t+k})^{-\alpha} + \pi\int_{g_d}^{g_u}(1+g_{t+k})^{-\alpha}dG(g_{t+k})} \quad \text{(A13)}$$

and

$$D_{t+k}^{*} = \sum_{\mathrm{s}=0}^{\mathrm{k}} D_{t+s}\frac{(1+\rho)}{(1-\pi)(1+g_{t+s})^{-\alpha} + \pi\int_{g_d}^{g_u}(1+g_{t+s})^{-\alpha}dG(g_{t+s})}. \quad \text{(A14)}$$

In addition, we know from the pricing kernel that:

$$\mathrm{E}_t\left[\beta\left(\frac{D_{t+1}}{D_t}\right)^{-\alpha}\frac{(1+\rho)}{(1-\pi)(1+g_{t+k})^{-\alpha} + \pi\int_{g_d}^{g_u}(1+g_{t+k})^{-\alpha}dG(g_{t+k})}\right] = 1. \quad \text{(A15)}$$

Using equation (A15) and adding $D_{t+k}^{CI^*}$ to both sides of equation (A12), we obtain:

$$S_{t+k}^{CI^*} + D_{t+k}^{*} = \mathrm{E}_{t+k}\left[\beta\left(\frac{D_{t+\mathrm{k}+1}}{D_{t+k}}\right)^{-\alpha}\frac{(1+\rho)}{(1-\pi)(1+g_{t+k})^{-\alpha} + \pi\int_{g_d}^{g_u}(1+g_{t+k})^{-\alpha}dG(g_{t+k})}(S_{t+k}^{CI^*} + D_{t+k+1}^{*})\right]. \quad \text{(A16)}$$

Therefore, we demonstrate that $S_{t+k}^{CI^*} + D_{t+k}^*$ follows a martingale under the conditional probability measure; and thus the risk-neutral density is:

$$\hat{p}_t(S_{t+k}^{CI}) = \beta\left(\frac{D_{t+1}}{D_t}\right)^{-\alpha} \frac{(1+\rho)}{(1-\pi)(1+g_{t+k})^{-\alpha} + \pi\int_{g_d}^{g_u}(1+g_{t+k})^{-\alpha}dG(g_{t+k})} p_t(D_{t+k}). \tag{A17}$$

Consequently, the one-period state-price density can be written as:

$$\begin{aligned}\tilde{p}_t(S_{t+k}^{CI}) &= \beta\left(\frac{D_{t+\mathrm{k}}}{D_t}\right)^{-\alpha} \frac{1}{1+r_{t+k}^{CI}} \\ &\cdot \frac{(1+\rho)}{(1-\pi)(1+g_{t+k})^{-\alpha} + \pi\int_{g_d}^{g_u}(1+g_{t+k})^{-\alpha}dG(g_{t+k})} p_t(D_{t+k}) \\ &= \beta\left(\frac{D_{t+1}}{D_t}\right)^{-\alpha} p_t(D_{t+k})\end{aligned} \tag{A18}$$

where r_{t+k}^{CI} is the one-period risk-free interest rate. Additionally, Pliska (1997) shows that if the risk-neutral measure on a single period model is unique and exists, it is a sufficient condition to have a unique risk-neutral measure on an infinite period model. The infinite period model risk-neutral measure can be obtained using the independence of breaks on the mean dividend growth rates and by taking all paths that could guide to a particular state in $t+\tau$ periods. In this context, $p_t^{CI}(S_{t+\tau}^{CI})$ is the state price density of all paths that lead to the state in which the dividend is $D_{t+\tau}$, while the expected value of $D_{t+\tau}$ is:

$$\mathrm{E_t}[D_{t+\tau}] = D_t \mathrm{E_t}\left[\frac{D_{t+1}}{D_t}\mathrm{E}_{t+1}\left[\left(\frac{D_{t+2}}{D_{t+1}}\right)\ldots \mathrm{E}_{t+\tau-1}\left[\left(\frac{D_{t+\tau}}{D_{t+\tau-1}}\right)\right]\right]\right]. \tag{A19}$$

Furthermore, using the independence of $\{\varepsilon_{t+i}\}_{i=1}^{\tau}$ and $\{g_{t+i-1}\}_{i=1}^{\tau}$ we have:

$$\mathrm{E_t}[D_{t+\tau}] = D_t \mathrm{E_t}\left[\exp\left(\sqrt{\tau}\sigma\varepsilon_{t+\tau} - \tau\sigma^2/2\right)\prod_{i=1}^{\tau}(1+g_{t+i-1})\right]. \tag{A20}$$

Lets z be the number of breaks between t and $t+\tau$ that is a random variable drawn from a Binomial distribution, $\varphi(z|\tau,\pi)$, with parameters τ and π; while $\{h_i\}_{i=0}^{z}$ are the time periods between breaks which are also random variables that follow geometric distributions with parameter π, $\eta(h_i|\pi)$, where $\tau = \sum_{i=0}^{z} h_i$. Then, in each path:

$$D_{t+\tau}^{CI} = D_t \exp\left(\sqrt{\tau}\sigma\varepsilon_{t+\tau} - \tau\sigma^2/2\right) \cdot \prod_{i=1}^{z+1}(1+g_{t+v_{i-1}})^{h_i} \tag{A21}$$

where $\left\{g_{t+h_i}\right\}_{i=1}^{z}$ are drawn from a univariate density $g_{t+h_{i-1}} \sim G(\cdot)$ and pdf $\varrho(g_{t+h_i})$ defined on the support $[g_d, g_u]$; while $g_{t+h_0} = g_t$ and $g_{t+\tau} = g_{t+h_z}$. Consequently,

$$\begin{aligned} p_t(D_{t+k}) = \phi(\varepsilon_{t+\tau}|0,\sigma)\varphi(z|\tau,\pi)\eta(h_0|\pi)\Big(\eta(h_1|\pi)\varrho\left(g_{t+h_1}\right)\cdot \ldots \\ \cdot \eta(h_z|\pi)\varrho\left(g_{t+h_z}\right)\Big) \end{aligned} \tag{A22}$$

and thus from equation (A18):

$$\begin{aligned} \tilde{p}_t(S_{t+k}^{CI}) = \beta^{\tau}\left(\frac{D_{t+\tau}}{D_t}\right)^{-\alpha}\phi(\varepsilon_{t+\tau}|0,\sigma)\varphi(z|\tau,\pi)\eta(h_0|\pi)\Big(\eta(h_1|\pi)\varrho\left(g_{t+h_1}\right)\cdot \ldots \\ \cdot \eta(h_z|\pi)\varrho\left(g_{t+h_z}\right)\Big). \end{aligned} \tag{A23}$$

□

Appendix B

We use data from the U.S. option market over the period between 1996 and 2007 to provide a comparison with the results obtained in the simulations using our Bayesian learning model. We include call equity options and call S&P 500 index options which are American and European style, respectively. We obtain the data from the OptionMetrics database that reports daily closing bid and ask quotes, implied volatilities, maturities, strike prices, underlying asset prices, and the risk-free term-structure of interest rates; where option prices correspond to bid-ask midpoints. In relation to equity options, we select only options in which their underlying stocks pay

dividends. We choose the 150 options with the highest volume which have been continuously traded in the sample period. We get option market data only on Wednesdays in a similar way to our simulations. Afterwards, we apply four exclusionary criteria in order to filter out observations that contain noisy data and that may hardly be thought of expressions of well-functioning markets. First, we eliminate all observations that violate basic no-arbitrage bounds. Second, we delete all contracts with less than six trading days and more than one year to expiration as their prices are usually noisy. Third and similar to Gonçalves and Guidolin (2006), we exclude contracts with prices lower than \$0.30 for equity options and \$3/8 for S&P 500 index options to avoid the effects of price discreteness on implied volatilities (i.e. in equity options the minimum tick is \$0.05 for trading prices lower than \$3, while for index options the smallest tick is \$1/16). Fourth, following Dumas *et al.* (1998) we exclude options contracts for which the moneyness is either less than 0.90 or in excess of 1.10, because deep in- and out-of-the money option contracts could cause additional noise in the analyses.

Appendix C

We use the test introduced by Chu *et al.* (1996) to estimate the probability of breaks on the mean dividend growth rate. Chu *et al.* (1996) present a dynamic test for structural breaks where market participants can identify contemporaneously a shift on a given date due to real-time features of their algorithm. Consider the dividend random walk process in equation (1). Let v be the minimum number of periods over which the drift is assumed to be constant, given that n is the number of periods from the last break (i.e. $\mu_{t-n+1} = \mu_{t-n+2} = \ldots = \mu_{t-n+v}$). Assuming that the representative agent starts detecting the presence of breaks after the span period v, Chu *et al.* (1996) propose the use of the following fluctuation detector in the case of a univariate location model:

$$\hat{Z}_t = n\hat{s}_0^{-1}(\hat{\mu}_t - \hat{\mu}_v) \qquad \text{(C1)}$$

where $\hat{\mu}_t$ and $\hat{\mu}_v$ are the parameter estimates at time t and v. We defined $\boldsymbol{\xi}_t$ as the vector of signals about μ_t in equation (10); therefore $\hat{\mu}_t = \bar{\xi}_t = (1/n)\sum_{i=t-n+1}^{t} \xi_i$ and $\hat{\mu}_v = \bar{\xi}_v = (1/v)\sum_{i=t-n+1}^{t-n+v} \xi_i$, while $\hat{s}_0 = (v^{-1}\sum_{i=t-n+1}^{t-n+v}(\xi_i - \hat{\mu}_v)^2)^{0.5}$. Assuming a null hypothesis of no break, Chu *et al.* (1996) present asymptotic bounds for the statistic $|\hat{Z}_t|$:

$$\lim_{v\to\infty} P\left\{|\hat{Z}_t| \geq \sqrt{v}\left(\frac{n-v}{v}\right)\left[\left(\frac{n}{n-v}\right)\left[a^2 + \ln\left(\frac{n}{n-v}\right)\right]\right]^{\frac{1}{2}}\right\} \cong 2\big(1 - \Phi(a) + a\phi(a)\big). \tag{C2}$$

Here $\Phi(\cdot)$ and $\phi(\cdot)$ are the cdf and pdf of a standard normal random variable, respectively, while a is a constant related to the significance level of the test. Consequently, the intuition behind this test is that given a significance level, an agent could start the calculation of $\hat{Z}_t$ recursively and in real-time after v signals received from the previous break to detect a new one. The testing process starts again after the detection of the new break. In this paper we assume that dividends are paid out daily, which is true for wide market indexes. For that reason and with the objective of detecting breaks, we use daily dividend time series from the S&P 500 index between 1996 and 2007 which were deseasonalized and adjusted by the consumer price index. We set v=125 which represents six months of trading dates, and we use 5% significance. We detect eight breaks in the period between 1996 and 2007. Figure C1 shows the breaks detected in the sample period.

[Insert Figure C1 here]

Appendix D

In this appendix, we report additional parameter setups for the analyses presented in this study. Table DI to Table DIV show summary statistics of dividends, interest rates, stock prices, and short-term at-the-money option contract prices and their implied volatilities. These tables present the results of multiple subsets of parameter

combinations under three scenarios: no breaks; breaks and complete information; and breaks and incomplete information with learning. In Table DI and Table DII (Table DIII and Table DIV), we set the coefficient of relative risk aversion at 0.5 (5.0). Furthermore, Table DV and Table DVI show dynamic features of the level, slopes, and curvatures of the *IVS* in an economy under breaks and incomplete information with learning. These tables reports outcomes using two different parameters setups. Finally, Tables DVII and Tables DVIII report cross-sectional relationships of the *IVS* shape features also in an economy under breaks and incomplete information with learning. In Tables DVII and Tables DVIII, we present correlation analyses among the level, slopes, and curvatures of the *IVS*.

[Insert Table DI here]

[Insert Table DII here]

[Insert Table DIII here]

[Insert Table DIV here]

[Insert Table DV here]

[Insert Table DVI here]

[Insert Table DVII here]

[Insert Table DVIII here]

Appendix E

In this appendix, we report fitting properties of a deterministic *IVS* model type as in Dumas *et al.* (1998), using implied volatilities in an economy under breaks and incomplete information with learning. The implied volatility polynomial function used is:

$$IV(Mon,\tau) = b_0 + b_1 Mon + b_2 Mon^2 + b_3\left(\frac{\tau}{365}\right) + b_4\left(\frac{\tau}{365}\right)^2 + b_5 Mon\left(\frac{\tau}{365}\right) + \epsilon \quad \text{(E1)}$$

where $IV(Mon,\tau)$ is the implied volatility of a call option contract with moneyness Mon and time-to-maturity τ. Table EI presents coefficients estimated and fitting statistics using equation (E1) with average implied volatilities from the U.S. option market and using our Bayesian learning model with multiple parameter combinations. Table EI shows that the *IVS* generated by the Bayesian learning model can be characterised by an implied volatility polynomial function as in Dumas *et al.* (1998) in a similar way to the implied volatilities reported in option trading data.

[Insert Table EI here]

References

Abel, A., 1988, Stock prices under time-varying dividend risk: An exact solution in an infinite-horizon general equilibrium model, *Journal of Monetary Economics* 22, 375-393.

Bakshi, G., G. Panayotov, and G. Skoulakis, 2011, Improving the predictability of real economic activity and asset returns with forward variances inferred from option portfolios, *Journal of Financial Economics* 100, 475-495.

Beber, A., and M. W. Brandt, 2006, The effect of macroeconomic news on beliefs and preferences: Evidence from the options market, *Journal of Monetary Economics* 53, 1997-2039.

Beber, A., and M. W. Brandt, 2009, Resolving macroeconomic uncertainty in stock and bond markets, *Review of Finance* 13, 1-45.

Bernales, A., and M. Guidolin, 2011, Can we forecast the implied volatility surface dynamics of equity options?, Working paper, Banque de France.

Black, F., and M., Scholes, 1973, The pricing of options and corporate liabilities, *Journal of Political* Economy 81, 637-654.

Bai, J., R. Lumsdaine, and J. Stock, 1998, Testing for and Dating Common Breaks in Multivariate Time Series, *Review of Economic Studies*, 63, 395-432.

Busch ,T., B. J. Christensen, and M. Ø. Nielsen, 2011, The role of implied volatility in forecasting future realized volatility and jumps in foreign exchange, stock, and bond markets, *Journal of Econometrics* 160, 48-57.

Cecchetti, S. G., P. Lam, and N. C. Mark, 1990, Mean reversion in equilibrium asset prices, *American Economic Review* 80, 221-242.

Chalamandaris, G., and A.E. Tsekrekos, 2010, Predictable dynamics in implied volatility surfaces from OTC currency options, *Journal of Banking and Finance* 34, 1175-1188.

Chang, B. Y., P. Christoffersen, K. Jacobs, and G. Vainberg, 2009, Option-implied measures of equity risk, Working paper, McGill University.

Christensen, B. J., and N. Prabhala, 1998, The Relation Between Implied and Realized Volatility, *Journal of Financial Economics*, 50, 125-150.

Christoffersen, P.F., S. Heston, and K. Jacobs, 2009, The shape and term structure of the index option smirk: Why multifactor stochastic volatility models work so well, *Management Science* 55, 1914-1932.

Chu, C. S. J. , M. Stinchcombe, and H. White, 1996, Monitoring structural change, *Econometrica* 64, 1045-1065.

Cremers, M., and D. Weinbaum, 2010, Deviations from put-call parity and stock return predictability, *Journal of Financial and Quantitative Analysis* 45, 335-367.

Das, S., and R. Sundaram, 1999, Of smiles and smirks: A term structure perspective, *Journal of Financial and Quantitative Analysis* 34, 211-239.

David, A., and P. Veronesi, 2002, Option prices with uncertain fundamentals, Working paper, University of Chicago.

Dennis, P., and S. Mayhew, 2002, Risk-neutral skewness: Evidence from stock options, *Journal of Financial and Quantitative Analysis* 37, 471-493.

Donders, M., R. Kouwenberg, and T. Vorst, 2000, Options and earnings announcements: An empirical study of volatility, trading volume, open interest, and liquidity, *European Financial Management* 6, 149–172.

Driessen, J., P. J. Maenhout, and G. Vilkov, 2009, The price of correlation risk: Evidence from equity options, *Journal of Finance* 64, 1377-1406.

Duan, J. C., and J. G. Simonato, 2001, American option pricing under GARCH by a Markov chain approximation, *Journal of Economic Dynamics and Control* 25, 1689-1718.

Duan, J. C., and W. Zhang, 2010, Forward-looking market risk premium, Working paper, National University of Singapore.

Dubinsky, A., and M. Johannes, 2006, Earnings announcements and equity options, Working paper, Columbia University.

Dumas, B., J. Fleming, and R. Whaley, 1998, Implied volatility functions: Empirical tests, *Journal of Finance* 53, 2059-2106.

Ederington, L., and J. H. Lee, 1996, The creation and resolution of market uncertainty: The impact of information releases on implied volatility, *Journal of Financial and Quantitative Analysis* 31, 513-539.

Engle, R., 1982, Autoregressive conditional heteroskedasticity with estimates of the variance of United Kingdom inflation, *Econometrica* 50, 987-1007.

Fengler, M.R., W.K. Härdle, and E. Mammen, 2007, A semiparametric factor model for implied volatility surface dynamics, *Journal of Financial Econometrics* 5, 189-218.

Gonçalves, S., and M. Guidolin, 2006, Predictable dynamics in the S&P 500 index options implied volatility surface, *Journal of Business* 79, 1591-1635.

Goyal, A., and A. Saretto, 2009, Cross-section of option returns and volatility, *Journal of Financial Economics* 94, 310-326.

Granger, C. and N. Hyung, 2004, Occasional structural breaks and long memory with an application to the S&P 500 absolute stock returns, *Journal of Empirical Finance* 3, 399-421.

Guidolin, M., and A. Timmermann, 2003, Option prices under Bayesian learning: Implied volatility dynamics and predictive densities, *Journal of Economic Dynamics and Control* 27, 717-769.

Harvey, C. R., and R. E. Whaley, 1992, Market volatility prediction and the efficiency of the S&P 100 index option market, *Journal of Financial Economics* 31, 43-73.

Heston, S., and S. Nandi, 2000, A closed-form GARCH option valuation model, *Review of Financial Studies* 13, 585-625.

Huang, C. F., and R. H. Litzenberger, 1988, *Foundations for Financial Economics* (North-Holland, The Netherlands).

Kleidon, A. W., 1986, Variance bounds tests and stock price valuation models, *Journal of Political Economy* 94, 953-1001.

Konstantinidi, E., G. Skiadopoulos, and E. Tzagkaraki, 2008, Can the evolution of implied volatility be forecasted? Evidence from European and US implied volatility indices, *Journal of Banking and Finance* 32, 2401-2411.

Kostakis, A., N. Panigirtzoglou, G. Skiadopoulos, 2011. Market timing with option-implied distributions: A forward-looking approach, *Management Science*, forthcoming.

Leisch, F., K. Hornik, and C. M. Kuan, 2000, Monitoring structural changes with the generalized fluctuation test, *Econometric Theory* 16, 835-854.

Lettau, M., and S. Van Nieuwerburgh, 2008, Reconciling the return predictability evidence, *Review of Financial Studies* 21, 1607-1652.

Lucas, R., 1978, Asset prices in an exchange economy, *Econometrica* 46, 1429-1445.

Ni, S. X., J. Pan, and A. M. Poteshman, 2008, Volatility information trading in the option market, *Journal of Finance* 63, 1059–1091.

Pastor, L., and R. F. Stambaugh, 2001, The equity premium and structural breaks, *Journal of Finance* 56, 1207-1239.

Patell, J. M., and M. A. Wolfson, 1979, Anticipated information releases reflected in call option prices, *Journal of Accounting and Economics* 1, 117–140.

Patell, J. M., and M. A. Wolfson, 1981, The ex ante and ex post price effects of quarterly earnings announcements reflection in option and stock prices, *Journal of Accounting Research* 19, 434-458.

Pliska, S. R., 1997, *Introduction to Mathematical Finance* (Blackwell, Oxford).

Rubinstein, M., 1985, Nonparametric tests of alternative option pricing models using all reported trades and quotes on the 30 most active CBOE option classes from August 23, 1976 through August 31, 1978, *Journal of Finance* 40, 455-480.

Shaliastovich, I., 2008, Learning, confidence and option prices, Working paper, Duke University.

Siegel, A. F., 1995, Measuring systematic risk using implicit beta, *Management Science* 41,124-128.

Timmermann, A., 1993, How learning in financial markets generates excess volatility and predictability of excess returns, *Quarterly Journal of Economics* 108, 1135-1145.

Timmermann, A., 1996, Excess volatility and predictability of stock prices in autoregressive dividend models with learning, *Review of Economic Studies*, 63, 523-557.

Timmermann, A., 2001, Structural breaks, incomplete information, and stock prices. *Journal of Business and Economic Statistics* 19, 299-314.

Whaley, R., and J. Cheung, 1982, Anticipation of quarterly earnings announcements: A test of option market efficiency, *Journal of Accounting and Economics* 4, 57–83.

Xing, Y., X. Zhang, and R. Zhao, 2010, What does individual option volatility smirk tell us about future equity returns?, *Journal of Financial and Quantitative Analysis* 45, 641-662.

Yan, S., 2011, Jump risk, stock returns, and slope of implied volatility smile, *Journal of Financial Economics* 99, 216-233.

Figures

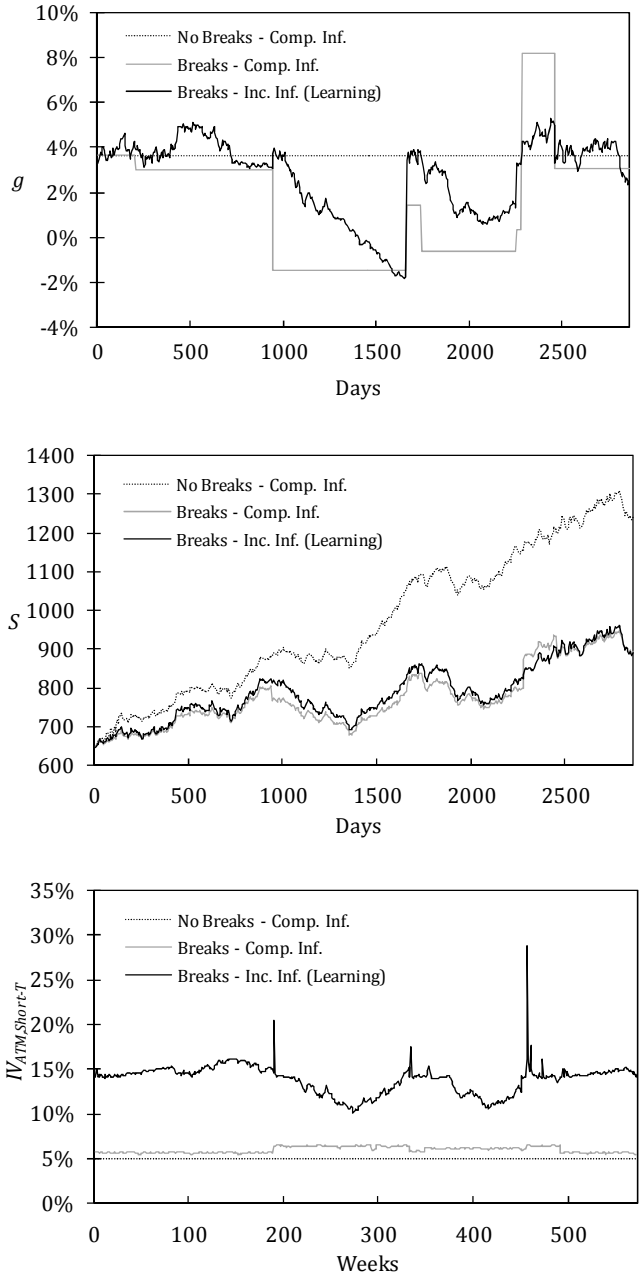

Figure 1. Evolutions of mean dividend growth rates, stock prices, and at-the-money short-term implied volatilities under three assumptions about the investor's expectations. The figure shows the outcome of one of the simulations reporting the evolutions over 12 years of the mean dividend growth rates (g), stock prices (S), and at-the-money short-term implied volatilities ($IV_{ATM,Short\text{-}T}$) under three scenarios: no breaks; breaks and complete information; and breaks and incomplete information with learning. $IV_{ATM,Short\text{-}T}$ is the implied volatility corresponding to a call option contract with 30-days to the expiration date (calendar days) and at-the-money. Given that the simulations replicate option prices in a realistic way, where there are not always exactly 30-days at-the-money option contracts, we calculate $IV_{ATM,Short\text{-}T}$ by simple linear interpolation using the four contracts around the 30-days time-to-maturity and with closest strike price to S. The assumed parameters are: α=0.2; π=66.7%; ρ=8.9%; σ=5.0%; g_u=8.8%; and g_u=-1.5%.

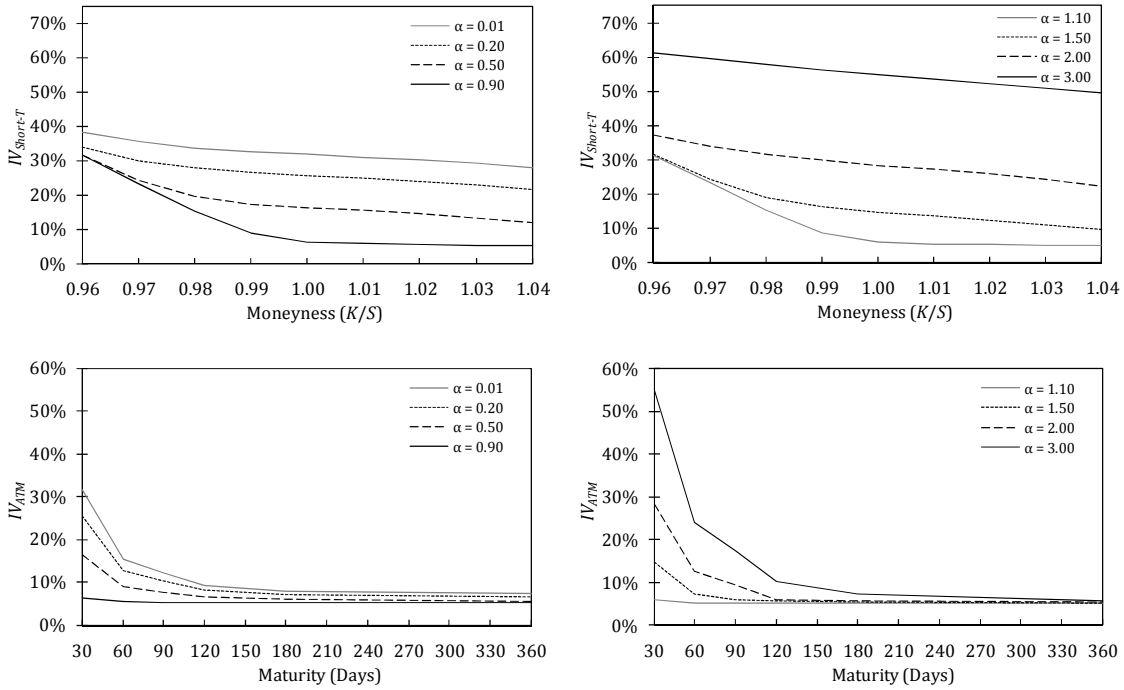

Figure 2. Sensitivity analysis in an economy with learning using diverse relative risk aversions regarding the average behaviour of the implied volatility surface one month after a break. The figure presents the average behaviour, *one month* after a break in g_t, of implied volatilities in an economy under breaks and incomplete information with learning. This figure shows implied volatilities on the moneyness dimension using short-term option contracts (upper windows) and the implied volatilities on the maturity dimension using at-the money option contracts (lower windows). $IV_{Short\text{-}T}$ (IV_{ATM}) represents the implied volatilities corresponding to call option contracts with 30-days to the expiration date (strike prices equal to S). Given that the simulations replicate option prices in a realistic way, where there are not always exactly 30-days or at-the-money option contracts, we calculate $IV_{Short\text{-}T}$ (IV_{ATM}) by simple linear interpolation using the two contracts around the 30-days time-to-maturity (closest strike price to S). The assumed parameters are: π=66.7%; ρ=8.9%; σ=5.0%; g_u=8.8%; and g_u=-1.5%.

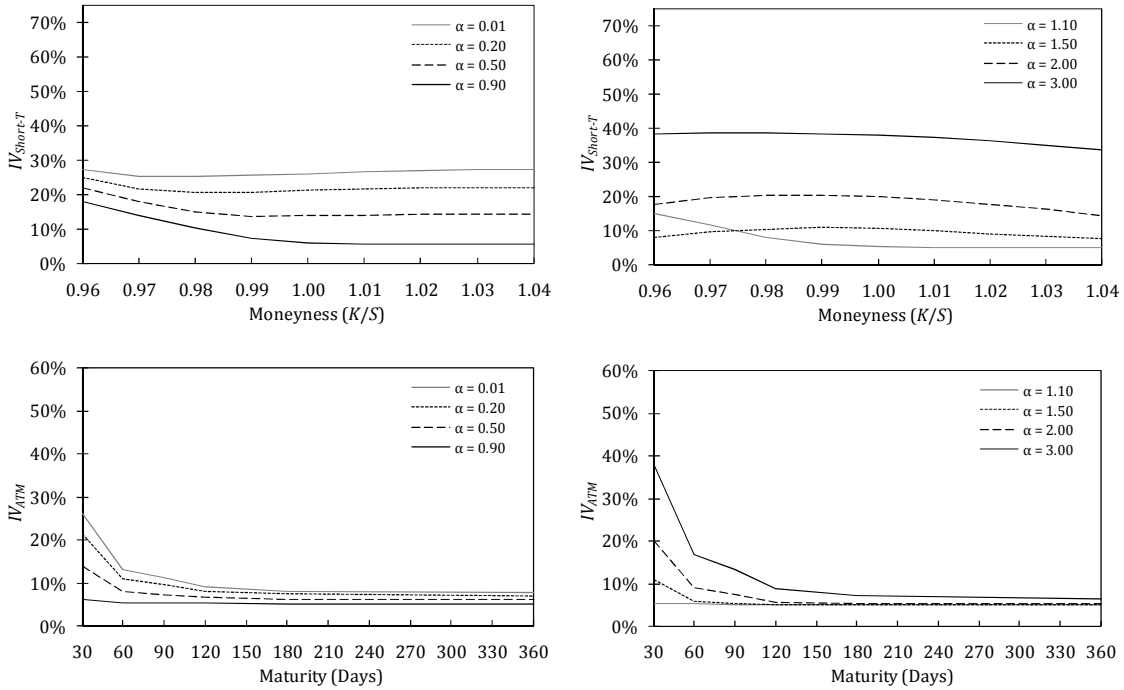

Figure 3. Sensitivity analysis in an economy with learning using diverse relative risk aversions regarding the average behaviour of the implied volatility surface 12 months after a break. The figure presents the average behaviour, *one year* after a break in g_t, of implied volatilities in an economy under breaks and incomplete information with learning. This figure shows implied volatilities on the moneyness dimension using short-term option contracts (upper windows) and the implied volatilities on the maturity dimension using at-the money option contracts (lower windows). $IV_{Short\text{-}T}$ and IV_{ATM} are defined in Figure 2. The assumed parameters are: π=66.7%; ρ=8.9%; σ=5.0%; g_u=8.8%; and g_u=-1.5%.

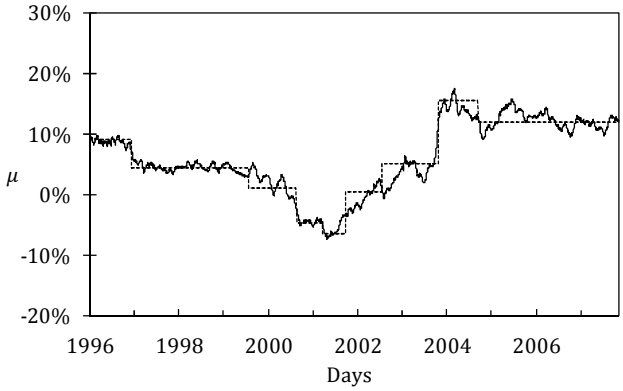

Figure C1. Structural breaks on the drift of the random walk process presented in equation (1). The solid line represents the dividend drift calculated with a rolling window of 125 trading days using log-return dividends from the S&P 500 index which were deseasonalized and adjusted by the consumer price index to obtain real dividends between 1996 and 2007. The dotted line shows structural breaks on the dividend drift. Breaks were detected in December 1996, August 1999, September 2000, April 2001, October 2001, August 2002, November 2003, and October 2004.

Tables

Table I
Summary Statistics of the Simulations under Three Assumptions on Investor's Expectations

The table contains summary statistics of the main variables in the simulations performed in our study using one parameter setup (additional summary statistics using diverse parameter combinations are presented in Table II and appendix D). The summary statistics are obtained under three scenarios: no breaks; breaks and complete information; and breaks and incomplete information with learning. The variables g, S, and $IV_{ATM,Short\text{-}T}$ are defined in Figure 1. *Div* is the daily dividend simulated while $r_{f,1\ day}$ is the one-day risk-free interest rate. $Call_{ATM,Short\text{-}T}$ is the price of a call option contract with 30-days to the expiration date (calendar days) and at-the-money. Given that the simulations replicate option prices in a realistic way, where there are not always exactly 30-days at-the-money option contracts, we calculate $Call_{ATM,Short\text{-}T}$ by simple linear interpolation using the four contracts around the 30-days time-to-maturity and with closest strike price to S.

Scenario	Variable	Mean	Median	Std. Dev.	Skewness	Excess Kurtosis	Min.	Max.
			α =0.2					
		π =66.7%, ρ =8.9%, σ =5.0%, g_u =8.8%, and g_d =-1.5%						
No Breaks - Comp. Inf.	*Div*	0.17	0.17	0.03	1.12	1.74	0.10	0.37
	g	3.65%	3.65%	0.00%	NA	NA	3.65%	3.65%
	$r_{f,\ 1\ day}$	9.68%	9.68%	0.00%	NA	NA	9.68%	9.68%
	S	813.22	761.05	153.29	1.12	1.74	109.43	1301.20
	$Call_{ATM,Short\text{-}T}$	4.39	4.30	1.57	0.38	-0.07	1.01	11.95
	$IV_{ATM,Short\text{-}T}$	5.00%	5.00%	0.00%	NA	NA	5.00%	5.00%
Breaks - Comp. Inf.	*Div*	0.18	0.17	0.04	1.28	1.92	0.11	0.38
	g	3.66%	3.65%	2.96%	0.00	-1.21	-1.49%	8.78%
	$r_{f,\ 1\ day}$	9.67%	9.75%	0.53%	-0.05	-0.90	9.29%	10.01%
	S	814.27	768.34	174.55	1.23	1.69	446.67	1678.97
	$Call_{ATM,Short\text{-}T}$	5.42	5.21	2.08	0.66	0.97	1.02	16.81
	$IV_{ATM,Short\text{-}T}$	5.75%	5.82%	0.31%	0.76	0.01	5.10%	7.44%
Breaks - Inc. Inf. (Learning)	*Div*	0.18	0.17	0.04	1.28	1.92	0.11	0.38
	g	3.64%	3.60%	1.62%	0.08	-0.16	-0.52%	8.33%
	$r_{f,\ 1\ day}$	9.67%	9.56%	0.29%	0.04	-0.15	9.31%	10.03%
	S	814.10	769.82	173.25	1.25	1.84	449.06	1730.23
	$Call_{ATM,Short\text{-}T}$	12.75	12.34	3.12	1.24	9.53	2.93	91.95
	$IV_{ATM,Short\text{-}T}$	19.24%	19.62%	3.60%	0.93	3.23	7.13%	74.11%

Table II
Summary Statistics of the Simulations under Three Assumptions on Investor's Expectations

The table contains summary statistics of the main variables in the simulations performed in our study using one parameter setup (additional summary statistics using diverse parameter combinations are presented in Table I and appendix D). The summary statistics are obtained under three scenarios: no breaks; breaks and complete information; and breaks and incomplete information with learning. The variables g, S, and $IV_{ATM,Short\text{-}T}$ are defined in Figure 1, while Div, $r_{f,1\ day}$, and $Call_{ATM,Short\text{-}T}$ are defined in Table I.

Scenario	Variable	Mean	Median	Std. Dev.	Skewness	Excess Kurtosis	Min.	Max.
			α=0.2					
		π=66.7%, ρ=9.6%, σ=30.0%, g_u=9.5%, and g_d=-5.0%						
No Breaks - Comp. Inf.	Div	0.18	0.13	0.16	2.46	8.97	0.00	1.64
	g	2.25%	2.25%	0.00%	NA	NA	2.25%	2.25%
	$r_{f,\,1\,day}$	10.09%	10.09%	0.00%	NA	NA	10.09%	10.09%
	S	698.66	501.26	626.41	2.46	9.07	18.47	6023.90
	$Call_{ATM,Short\text{-}T}$	18.32	13.93	12.83	0.80	-0.17	0.13	210.41
	$IV_{ATM,Short\text{-}T}$	30.00%	30.00%	0.00%	NA	NA	30.00%	30.00%
Breaks - Comp. Inf.	Div	0.18	0.13	0.17	2.56	9.07	0.00	1.66
	g	2.27%	2.25%	4.17%	0.01	-1.19	-4.94%	9.48%
	$r_{f,\,1\,day}$	10.08%	10.11%	0.79%	-0.09	-0.95	9.52%	10.52%
	S	700.93	504.80	676.20	2.62	9.67	18.91	6797.87
	$Call_{ATM,Short\text{-}T}$	26.13	23.30	18.44	1.28	2.35	1.60	241.42
	$IV_{ATM,Short\text{-}T}$	31.63%	31.28%	0.83%	0.83	0.77	30.06%	33.20%
Breaks - Inc. Inf. (Learning)	Div	0.18	0.13	0.17	2.56	9.07	0.00	1.66
	g	2.24%	2.22%	2.68%	0.25	-0.35	-1.73%	9.23%
	$r_{f,\,1\,day}$	10.04%	10.04%	0.13%	0.21	-0.31	9.79%	10.55%
	S	699.91	503.95	673.46	2.60	9.34	19.96	6990.88
	$Call_{ATM,Short\text{-}T}$	35.13	34.71	22.62	3.36	15.78	1.74	424.78
	$IV_{ATM,Short\text{-}T}$	43.28%	42.19%	5.40%	4.23	9.15	30.79%	221.23%

Table III
The Learning Process Effects on the Implied Volatility Surface Dynamics

The table contains time series statistics of the level, slopes, and curvatures of the *IVS* on both moneyness and maturity dimensions in an economy under breaks and incomplete information with learning. This table shows outcomes using two parameter setups (additional time series statistics using diverse parameter combinations are presented in appendix D). $IV_{ATM,Short\text{-}T}$ is defined in Figure 1. We define $Slope_{Mon}$ ($Slope_{Mat}$) as the average of numerical first derivatives using all pairs of moneyness-consecutive 30-days (maturity-consecutive at-the-money) implied volatilities. $Curv_{Mon}$ ($Curve_{Mat}$) is the average of numerical second derivatives using all trios of moneyness-consecutive 30-days (maturity-consecutive at-the-money) implied volatilities. Serial Correlation is the statistic of the first order Ljung-Box test. The ARCH(1) and ARCH(3) statistics are the values of the LM test for ARCH effects suggested by Engle (1982) using one and three lags, respectively. The percentage of the simulations with significant statistics of the respective diagnostic tests is reported in parentheses at 10% significance.

Variable	Mean	Std. Dev.	Skewness	Excess Kurtosis	Serial Correlation	ARCH(1)	ARCH(3)
				α=0.2			
	Panel A: π=66.7%, ρ=8.9%, σ=5.0%, g_u=8.8%, and g_d=-1.5%						
$IV_{ATM,Short\text{-}T}$	19.24%	3.60%	0.93	3.23	55.83	41.05	42.57
					(98.80)	(91.30)	(91.10)
$Slope_{Mon}$	-0.35	0.14	-0.31	2.35	18.04	5.66	10.10
					(78.50)	(39.30)	(42.70)
$Curv_{Mon}$	30.90	20.99	0.13	11.62	12.80	4.04	7.60
					(62.20)	(28.20)	(29.40)
$Slope_{Mat}$	-0.31	0.08	-0.02	1.81	53.16	37.03	38.76
					(98.80)	(87.50)	(86.00)
$Curv_{Mat}$	3.28	1.12	0.21	4.47	47.56	29.66	31.61
					(98.80)	(84.80)	(81.90)
	Panel B: π=66.7%, ρ=9.6%, σ=30.0%, g_u=9.5%, and g_d=-5.0%						
$IV_{ATM,Short\text{-}T}$	43.28%	5.40%	4.23	9.15	50.46	39.74	38.31
					(93.30)	(88.70)	(90.30)
$Slope_{Mon}$	-0.19	0.15	-0.57	7.54	16.07	4.41	8.89
					(75.80)	(31.90)	(35.30)
$Curv_{Mon}$	2.87	2.40	0.44	17.60	9.37	2.86	7.23
					(53.40)	(27.80)	(26.20)
$Slope_{Mat}$	-0.31	0.09	-0.03	3.14	49.85	33.87	36.65
					(92.20)	(78.90)	(79.20)
$Curv_{Mat}$	3.53	1.72	0.62	6.38	44.38	27.61	26.48
					(92.20)	(77.90)	(78.30)

Table IV

Time Series Statistics of Implied Volatility Surface Using Option Market Data

The table contains time series statistics of the level, slopes, and curvatures of the *IVS* on both moneyness and maturity dimensions using U.S. option market data over the period between 1997 and 2007. Panel A (Panel B) reports time series statistics of the *IVS* shape features using S&P 500 index options (150 equity options in which the underlying stocks pay dividends). The option market data used is explained in appendix B. $IV_{ATM,Short\text{-}T}$ is defined in Figure 1, while $Slope_{Mon}$, $Curv_{Mon}$, $Slope_{Mat}$, and $Curv_{Mon}$ are defined in Table III. Serial Correlation is the statistic of the first order Ljung-Box test. The ARCH(1) and ARCH(3) statistics are the values of the LM test for ARCH effects suggested by Engle (1982) using one and three lags, respectively. The percentage of options with significant statistics of the respective diagnostic tests is reported in parentheses at 10% significance.

Variable	Mean	Std. Dev.	Skewness	Excess Kurtosis	Serial Correlation	ARCH(1)	ARCH(3)
	Panel A: S&P 500 Options						
$IV_{ATM,Short\text{-}T}$	16.65%	5.90%	0.71	0.42	422.82	266.05	267.56
					(100.00)	(100.00)	(100.00)
$Slope_{Mon}$	-0.64	0.21	-0.48	0.69	82.70	15.21	18.21
					(100.00)	(100.00)	(100.00)
$Curv_{Mon}$	13.84	14.40	0.08	7.38	14.02	0.35	15.42
					(100.00)	(0.00)	(100.00)
$Slope_{Mat}$	0.03	0.07	-0.60	2.48	205.68	126.97	141.14
					(100.00)	(100.00)	(100.00)
$Curv_{Mat}$	-0.12	0.60	0.24	5.06	23.02	0.18	36.69
					(100.00)	(0.00)	(100.00)
	Panel B: Equity Options						
$IV_{ATM,Short\text{-}T}$	40.34%	5.63%	0.67	0.86	59.33	29.06	31.39
					(98.00)	(74.00)	(69.33)
$Slope_{Mon}$	-0.21	0.70	1.03	26.31	4.72	2.18	7.02
					(32.67)	(13.33)	(17.33)
$Curv_{Mon}$	2.62	10.61	-0.35	11.50	1.85	2.64	4.98
					(18.67)	(15.33)	(18.67)
$Slope_{Mat}$	-0.04	0.09	-0.90	2.82	36.23	12.44	14.94
					(96.00)	(60.00)	(57.33)
$Curv_{Mat}$	0.08	0.55	0.59	3.92	17.39	7.38	10.40
					(90.00)	(48.67)	(44.67)

Table V

The Learning Impacts on Cross-Sectional Relationships of Implied Volatility Surface Features

The table contains correlation analyses of the level, slopes, and curvatures of the *IVS* in an economy under breaks and incomplete information with learning. This table shows outcomes using two parameter setups (additional correlation analyses using diverse parameter combinations are presented in appendix D). $IV_{ATM,Short\text{-}T}$ is defined in Figure 1, while $Slope_{Mon}$, $Curv_{Mon}$, $Slope_{Mat}$, and $Curv_{Mon}$ are defined in Table III. The percentage of the simulations with significant statistics of the respective diagnostic tests is reported in parentheses at 10% significance.

Variable	$IV_{ATM,Short\text{-}T}$	$Slope_{Mon}$	$Curv_{Mon}$	$Slope_{Mat}$	$Curv_{Mat}$
			α=0.2		
	Panel A: π=66.7%, ρ=8.9%, σ=5.0%, g_u=8.8%, and g_d=-1.5%				
$IV_{ATM,Short\text{-}T}$	1.00				
	(100.00)				
$Slope_{Mon}$	-0.38	1.00			
	(80.10)	(100.00)			
$Curv_{Mon}$	-0.14	-0.47	1.00		
	(67.90)	(81.30)	(100.00)		
$Slope_{Mat}$	-0.96	0.32	0.17	1.00	
	(99.20)	(76.40)	(64.50)	(100.00)	
$Curv_{Mat}$	0.89	-0.28	-0.15	-0.91	1.00
	(98.90)	(74.80)	(70.30)	(98.50)	(100.00)
	Panel B: π=66.7%, ρ=9.6%, σ=30.0%, g_u=9.5%, and g_d=-5.0%				
$IV_{ATM,Short\text{-}T}$	1.00				
	(100.00)				
$Slope_{Mon}$	-0.35	1.00			
	(74.60)	(100.00)			
$Curv_{Mon}$	-0.12	-0.46	1.00		
	(66.90)	(79.70)	(100.00)		
$Slope_{Mat}$	-0.42	0.31	0.00	1.00	
	(89.90)	(72.40)	(58.90)	(100.00)	
$Curv_{Mat}$	0.38	-0.11	-0.09	-0.72	1.00
	(79.70)	(54.60)	(52.80)	(81.20)	(100.00)

Table VI

Cross-Sectional Relationships of Implied Volatility Surface Features Using Option Market Data

The table contains correlation analyses of the level, slopes, and curvatures of the *IVS* using U.S. option market data over the period between 1997 and 2007. Panel A (Panel B) reports a correlation analysis of the implied volatilities surface features using S&P 500 index options (150 equity options in which the underlying stocks pay dividends). The option market data used is explained in appendix B. $IV_{ATM,Short\text{-}T}$ is defined in Figure 1, while $Slope_{Mon}$, $Curv_{Mon}$, $Slope_{Mat}$, and $Curv_{Mon}$ are defined in Table III. The percentage of options with significant statistics of the respective diagnostic tests is reported in parentheses at 10% significance.

Variable	$IV_{ATM,Short\text{-}T}$	$Slope_{Mon}$	$Curv_{Mon}$	$Slope_{Mat}$	$Curv_{Mat}$
	Panel A: S&P 500 Options				
$IV_{ATM,Short\text{-}T}$	1.00				
	(100.00)				
$Slope_{Mon}$	-0.24	1.00			
	(100.00)	(100.00)			
$Curv_{Mon}$	-0.35	-0.09	1.00		
	(100.00)	(100.00)	(100.00)		
$Slope_{Mat}$	-0.40	0.00	0.27	1.00	
	(100.00)	(0.00)	(100.00)	(100.00)	
$Curv_{Mat}$	0.02	0.07	-0.05	-0.29	1.00
	(0.00)	(0.00)	(0.00)	(100.00)	(100.00)
	Panel B: Equity Options				
$IV_{ATM,Short\text{-}T}$	1.00				
	(100.00)				
$Slope_{Mon}$	-0.11	1.00			
	(46.67)	(100.00)			
$Curv_{Mon}$	-0.29	-0.11	1.00		
	(86.00)	(64.67)	(100.00)		
$Slope_{Mat}$	-0.57	0.28	0.06	1.00	
	(97.33)	(80.00)	(46.67)	(100.00)	
$Curv_{Mat}$	0.24	-0.25	0.03	-0.62	1.00
	(76.67)	(80.00)	(41.33)	(99.33)	(100.00)

Table DI
Summary Statistics of the Simulations under Three Assumptions on Investor's Expectations

The table contains summary statistics of the main variables in the simulations performed in our study using one parameter setup. The summary statistics are obtained under three scenarios: no breaks; breaks and complete information; and breaks and incomplete information with learning. The variables g, S, and $IV_{ATM,Short\text{-}T}$ are defined in Figure 1, while Div, $r_{f,1\ day}$, and $Call_{ATM,Short\text{-}T}$ are defined in Table I.

Scenario	Variable	Mean	Median	Std. Dev.	Skewness	Excess Kurtosis	Min.	Max.
			α=0.5					
		π=66.7%, ρ=8.9%, σ=5.0%, g_u=8.8%, and g_d=-1.5%						
No Breaks - Comp. Inf.	Div	0.17	0.17	0.03	1.12	1.74	0.10	0.37
	g	3.65%	3.65%	0.00%	NA	NA	3.65%	3.65%
	$r_{f,\,1\,day}$	10.87%	10.87%	0.00%	NA	NA	10.87%	10.87%
	S	677.92	630.32	129.27	1.12	1.74	98.31	1093.35
	$Call_{ATM,Short\text{-}T}$	3.73	3.64	1.38	0.34	-0.13	0.55	11.94
	$IV_{ATM,Short\text{-}T}$	5.00%	5.00%	0.00%	NA	NA	5.00%	5.00%
Breaks - Comp. Inf.	Div	0.18	0.17	0.04	1.28	1.92	0.11	0.38
	g	3.66%	3.65%	2.96%	0.00	-1.21	-1.49%	8.78%
	$r_{f,\,1\,day}$	10.88%	10.87%	1.32%	-0.06	-0.91	9.91%	11.66%
	S	683.44	645.19	143.97	1.25	1.77	382.30	1406.32
	$Call_{ATM,Short\text{-}T}$	4.53	4.32	1.80	0.69	0.59	0.68	13.49
	$IV_{ATM,Short\text{-}T}$	5.43%	5.58%	0.20%	0.64	0.87	5.04%	6.75%
Breaks - Inc. Inf. (Learning)	Div	0.18	0.17	0.04	1.28	1.92	0.11	0.38
	g	3.64%	3.60%	1.48%	0.08	-0.16	-0.52%	8.33%
	$r_{f,\,1\,day}$	10.86%	10.84%	0.72%	0.04	-0.17	10.08%	11.54%
	S	683.34	646.44	143.54	1.26	1.87	383.56	1437.51
	$Call_{ATM,Short\text{-}T}$	7.51	7.27	2.06	1.53	17.21	1.38	68.29
	$IV_{ATM,Short\text{-}T}$	13.91%	13.57%	2.53%	1.73	14.13	6.07%	56.78%

Table DII
Summary Statistics of the Simulations under Three Assumptions on Investor's Expectations

The table contains summary statistics of the main variables in the simulations performed in our study using one parameter setup. The summary statistics are obtained under three scenarios: no breaks; breaks and complete information; and breaks and incomplete information with learning. The variables g, S, and $IV_{ATM,Short\text{-}T}$ are defined in Figure 1, while Div, $r_{f,1\ day}$, and $Call_{ATM,Short\text{-}T}$ are defined in Table I.

Scenario	Variable	Mean	Median	Std. Dev.	Skewness	Excess Kurtosis	Min.	Max.
			α =0.5					
		π =66.7%, ρ =9.6%, σ =30.0%, g_u =9.5%, and g_d =-5.0%						
No Breaks - Comp. Inf.	Div	0.18	0.13	0.16	2.46	8.97	0.00	1.64
	g	2.25%	2.25%	0.00%	NA	NA	2.25%	2.25%
	$r_{f,\,1\,day}$	10.83%	10.83%	0.00%	NA	NA	10.83%	10.83%
	S	503.56	423.27	362.95	2.46	9.07	35.63	2812.15
	$Call_{ATM,Short\text{-}T}$	16.03	13.23	11.50	0.79	0.16	0.53	93.12
	$IV_{ATM,Short\text{-}T}$	30.00%	30.00%	0.00%	NA	NA	30.00%	30.00%
Breaks - Comp. Inf.	Div	0.18	0.13	0.17	2.56	9.07	0.00	1.66
	g	2.27%	2.25%	4.17%	0.01	-1.19	-4.94%	9.48%
	$r_{f,\,1\,day}$	10.87%	10.85%	1.88%	-0.05	-0.75	9.41%	12.11%
	S	508.52	425.48	388.35	2.27	7.46	47.79	3244.08
	$Call_{ATM,Short\text{-}T}$	22.06	18.65	17.36	1.02	2.51	3.96	101.40
	$IV_{ATM,Short\text{-}T}$	31.23%	31.60%	0.78%	0.31	1.24	30.64%	32.50%
Breaks - Inc. Inf. (Learning)	Div	0.18	0.13	0.17	2.56	9.07	0.00	1.66
	g	2.24%	2.22%	2.68%	0.25	-0.35	-1.73%	9.23%
	$r_{f,\,1\,day}$	10.81%	10.80%	0.31%	0.78	-0.38	10.07%	12.01%
	S	507.68	425.47	383.20	2.23	7.28	48.21	3218.93
	$Call_{ATM,Short\text{-}T}$	30.44	28.39	19.24	3.67	19.38	2.28	361.77
	$IV_{ATM,Short\text{-}T}$	36.81%	36.39%	5.30%	5.28	19.80	31.13%	241.62%

Table DIII
Summary Statistics of the Simulations under Three Assumptions about the Investor's Expectations

The table contains summary statistics of the main variables in the simulations performed in our study using one parameter setup. The summary statistics are obtained under three scenarios: no breaks; breaks and complete information; and breaks and incomplete information with learning. The variables g, S, and $IV_{ATM,Short\text{-}T}$ are defined in Figure 1, while Div, $r_{f,1\ day}$, and $Call_{ATM,Short\text{-}T}$ are defined in Table I.

Scenario	Variable	Mean	Median	Std. Dev.	Skewness	Excess Kurtosis	Min.	Max.
			α=5.0					
		π=66.7%, ρ=8.9%, σ=5.0%, g_u=8.8%, and g_d=-1.5%						
No Breaks - Comp. Inf.	Div	0.17	0.17	0.03	1.12	1.74	0.10	0.37
	g	3.65%	3.65%	0.00%	NA	NA	3.65%	3.65%
	$r_{f,\ 1\ day}$	30.28%	30.28%	0.00%	NA	NA	30.28%	30.28%
	S	216.72	201.33	37.52	1.12	1.74	38.94	321.86
	$Call_{ATM,Short\text{-}T}$	1.19	1.03	0.83	0.52	-0.78	0.01	4.23
	$IV_{ATM,Short\text{-}T}$	5.00%	5.00%	0.00%	NA	NA	5.00%	5.00%
Breaks - Comp. Inf.	Div	0.18	0.17	0.04	1.28	1.92	0.11	0.38
	g	3.66%	3.65%	2.96%	0.00	-1.21	-1.49%	8.78%
	$r_{f,\ 1\ day}$	30.35%	30.28%	13.22%	-0.04	-0.95	18.61%	40.27%
	S	218.97	209.28	47.93	1.29	2.66	121.79	554.54
	$Call_{ATM,Short\text{-}T}$	1.69	1.55	0.98	0.76	0.69	0.03	8.70
	$IV_{ATM,Short\text{-}T}$	8.62%	7.79%	0.88%	1.48	3.87	5.76%	14.65%
Breaks - Inc. Inf. (Learning)	Div	0.18	0.17	0.04	1.28	1.92	0.11	0.38
	g	3.64%	3.60%	1.62%	0.08	-0.16	-0.52%	8.33%
	$r_{f,\ 1\ day}$	30.21%	29.95%	7.15%	0.04	-0.17	20.97%	39.15%
	S	219.73	207.98	41.98	1.40	2.40	130.84	558.04
	$Call_{ATM,Short\text{-}T}$	10.69	10.40	2.77	2.78	12.46	1.85	52.30
	$IV_{ATM,Short\text{-}T}$	69.12%	68.22%	10.56%	2.45	5.38	19.00%	206.22%

Table DIV
Summary Statistics of the Simulations under Three Assumptions about the Investor's Expectations

The table contains summary statistics of the main variables in the simulations performed in our study using one parameter setup. The summary statistics are obtained under three scenarios: no breaks; breaks and complete information; and breaks and incomplete information with learning. The variables g, S, and $IV_{ATM,Short\text{-}T}$ are defined in Figure 1, while Div, $r_{f,1\ day}$, and $Call_{ATM,Short\text{-}T}$ are defined in Table I

Scenario	Variable	Mean	Median	Std. Dev.	Skewness	Excess Kurtosis	Min.	Max.
			α =5.0					
		π =66.7%, ρ =9.6%, σ =30.0%, g_u =9.5%, and g_d =-5.0%						
No Breaks - Comp. Inf.	Div	0.18	0.13	0.16	2.46	8.97	0.00	1.64
	g	2.25%	2.25%	0.00%	NA	NA	2.25%	2.25%
	$r_{f,\ 1\ day}$	22.50%	22.50%	0.00%	NA	NA	22.50%	22.50%
	S	206.85	191.62	144.10	2.46	9.07	22.04	1113.94
	$Call_{ATM,Short\text{-}T}$	6.34	5.26	4.52	0.73	-0.85	0.01	37.11
	$IV_{ATM,Short\text{-}T}$	30.00%	30.00%	0.00%	NA	NA	30.00%	30.00%
Breaks - Comp. Inf.	Div	0.18	0.13	0.17	2.56	9.07	0.00	1.66
	g	2.27%	2.25%	4.17%	0.01	-1.19	-4.94%	9.48%
	$r_{f,\ 1\ day}$	22.49%	22.41%	18.80%	-0.07	-0.89	6.79%	35.34%
	S	213.66	201.30	190.36	1.90	5.77	24.36	1660.59
	$Call_{ATM,Short\text{-}T}$	8.95	6.99	8.20	2.94	9.48	1.18	76.88
	$IV_{ATM,Short\text{-}T}$	45.85%	43.49%	2.29%	0.45	2.46	34.94%	47.29%
Breaks - Inc. Inf. (Learning)	Div	0.18	0.13	0.17	2.56	9.07	0.00	1.66
	g	2.24%	2.22%	2.68%	0.25	-0.35	-1.73%	9.23%
	$r_{f,\ 1\ day}$	22.66%	22.35%	3.09%	0.80	-0.41	14.01%	35.06%
	S	215.78	211.00	199.09	2.20	7.21	29.15	1688.65
	$Call_{ATM,Short\text{-}T}$	24.09	18.99	21.20	4.30	13.63	2.62	322.85
	$IV_{ATM,Short\text{-}T}$	141.10%	140.70%	23.90%	7.35	9.14	42.40%	346.40%

Table DV

The Learning Process Effects on the Implied Volatility Surface Dynamics

The table contains time series statistics of the level, slopes, and curvatures of the *IVS* on both moneyness and maturity dimensions in an economy under breaks and incomplete information with learning. This table shows outcomes using two parameter setups. $IV_{ATM,Short\text{-}T}$ is defined in Figure 1, while $Slope_{Mon}$, $Curv_{Mon}$, $Slope_{Mat}$, and $Curv_{Mon}$ are defined in Table III. Serial Correlation is the statistic of the first order Ljung-Box test. The ARCH(1) and ARCH(3) statistics are the values of the LM test for ARCH effects suggested by Engle (1982) using one and three lags, respectively. The percentage of the simulations with significant statistics of the respective diagnostic tests is reported in parentheses at 10% significance.

Variable	Mean	Std. Dev.	Skewness	Excess Kurtosis	Serial Correlation	ARCH(1)	ARCH(3)
				α=0.5			
	Panel A: π=66.7%, ρ=8.9%, σ=5.0%, g_u=8.8%, and g_d=-1.5%						
$IV_{ATM,Short\text{-}T}$	13.91%	2.53%	1.73	14.13	67.36	49.36	50.96
					(98.90)	(91.40)	(92.60)
$Slope_{Mon}$	-0.91	0.16	-0.46	5.41	20.49	6.19	10.72
					(79.20)	(40.60)	(45.40)
$Curv_{Mon}$	53.36	25.55	0.37	9.44	26.78	8.65	13.09
					(82.50)	(45.80)	(45.80)
$Slope_{Mat}$	-0.17	0.06	-0.09	4.31	66.18	47.52	49.49
					(98.80)	(91.40)	(89.50)
$Curv_{Mat}$	1.93	0.94	0.15	2.07	56.59	33.03	35.43
					(98.90)	(86.10)	(83.40)
	Panel B: π=66.7%, ρ=9.6%, σ=30.0%, g_u=9.5%, and g_d=-5.0%						
$IV_{ATM,Short\text{-}T}$	36.81%	5.30%	5.28	19.80	57.43	29.67	34.79
					(96.90)	(76.30)	(86.80)
$Slope_{Mon}$	-0.23	0.13	-0.43	8.05	19.90	4.95	9.26
					(78.40)	(38.40)	(41.10)
$Curv_{Mon}$	4.52	3.14	1.42	15.53	23.46	7.68	11.93
					(76.60)	(43.403)	(49.70)
$Slope_{Mat}$	-0.20	0.07	-0.10	7.14	61.83	45.21	42.88
					(95.30)	(89.10)	(80.30)
$Curv_{Mat}$	1.94	0.96	0.49	8.53	46.17	30.51	26.84
					(91.70)	(79.80)	(72.40)

Table DVI
The Learning Process Effects on the Implied Volatility Surface Dynamics

The table contains time series statistics of the level, slopes, and curvatures of the *IVS* on both moneyness and maturity dimensions in an economy under breaks and incomplete information with learning. This table shows outcomes using two parameter setups. $IV_{ATM,Short\text{-}T}$ is defined in Figure 1, while $Slope_{Mon}$, $Curv_{Mon}$, $Slope_{Mat}$, and $Curv_{Mon}$ are defined in Table III. Serial Correlation is the statistic of the first order Ljung-Box test. The ARCH(1) and ARCH(3) statistics are the values of the LM test for ARCH effects suggested by Engle (1982) using one and three lags, respectively. The percentage of the simulations with significant statistics of the respective diagnostic tests is reported in parentheses at 10% significance.

Variable	Mean	Std. Dev.	Skewness	Excess Kurtosis	Serial Correlation	ARCH(1)	ARCH(3)
				α =5.0			
	Panel A: π =66.7%, ρ =8.9%, σ =5.0%, g_u =8.8%, and g_d =-1.5%						
$IV_{ATM,Short\text{-}T}$	69.12%	10.56%	2.45	5.38	55.58	50.47	49.65
					(99.80)	(96.50)	(95.80)
$Slope_{Mon}$	-0.49	0.31	0.24	4.51	30.10	12.95	14.70
					(92.70)	(70.60)	(64.40)
$Curv_{Mon}$	-11.92	4.57	-0.46	4.52	10.08	5.04	6.94
					(67.80)	(41.60)	(35.30)
$Slope_{Mat}$	-1.24	0.38	-0.37	3.02	54.05	46.59	46.40
					(98.50)	(95.10)	(94.10)
$Curv_{Mat}$	12.17	2.53	0.15	5.90	48.90	35.08	36.28
					(98.70)	(92.10)	(90.60)
	Panel B: π =66.7%, ρ =9.6%, σ =30.0%, g_u =9.5%, and g_d =-5.0%						
$IV_{ATM,Short\text{-}T}$	141.10%	23.90%	7.35	9.14	49.04	36.19	41.22
					(96.40)	(89.40)	(87.30)
$Slope_{Mon}$	-0.20	0.29	0.83	6.67	27.99	10.91	13.07
					(77.80)	(62.70)	(62.80)
$Curv_{Mon}$	-4.37	7.34	-0.60	8.43	8.77	4.26	6.19
					(62.70)	(40.10)	(34.80)
$Slope_{Mat}$	-2.69	0.77	-0.34	5.69	49.90	33.18	36.74
					(94.40)	(91.10)	(89.20)
$Curv_{Mat}$	25.97	3.75	0.45	7.74	45.56	30.79	34.12
					(95.10)	(88.30)	(85.90)

Table DVII

The Learning Impacts on Cross-Sectional Relationships of Implied Volatility Surface Features

The table contains correlation analyses of the level, slopes, and curvatures of *IVS* in an economy under breaks and incomplete information with learning. This table shows outcomes using two parameter setups. $IV_{ATM,Short\text{-}T}$ is defined in Figure 1, while $Slope_{Mon}$, $Curv_{Mon}$, $Slope_{Mat}$, and $Curv_{Mon}$ are defined in Table III. The percentage of the simulations with significant statistics of the respective diagnostic tests is reported in parentheses at 10% significance.

Variable	$IV_{ATM,Short\text{-}T}$	$Slope_{Mon}$	$Curv_{Mon}$	$Slope_{Mat}$	$Curv_{Mat}$
			α=0.5		
	Panel A: π=66.7%, ρ=8.9%, σ=5.0%, g_u=8.8%, and g_d=-1.5%				
$IV_{ATM,Short\text{-}T}$	1.00				
	(100.00)				
$Slope_{Mon}$	-0.64	1.00			
	(96.40)	(100.00)			
$Curv_{Mon}$	0.21	-0.83	1.00		
	(68.90)	(96.90)	(100.00)		
$Slope_{Mat}$	-0.95	0.57	0.19	1.00	
	(98.70)	(94.10)	(68.60)	(100.00)	
$Curv_{Mat}$	0.91	-0.51	-0.18	-0.94	1.00
	(98.70)	(93.60)	(61.40)	(98.80)	(100.00)
	Panel B: π=66.7%, ρ=9.6%, σ=30.0%, g_u=9.5%, and g_d=-5.0%				
$IV_{ATM,Short\text{-}T}$	1.00				
	(100.00)				
$Slope_{Mon}$	-0.45	1.00			
	(91.40)	(100.00)			
$Curv_{Mon}$	0.19	-0.49	1.00		
	(65.30)	(94.90)	(100.00)		
$Slope_{Mat}$	-0.40	0.37	0.13	1.00	
	(84.30)	(78.60)	(54.60)	(100.00)	
$Curv_{Mat}$	0.34	-0.09	-0.14	-0.68	1.00
	(78.90)	(55.40)	(59.10)	(86.60)	(100.00)

Table DVIII

The Learning Impacts on Cross-Sectional Relationships of Implied Volatility Surface Features

The table contains correlation analyses of the level, slopes, and curvatures of *IVS* in an economy under breaks and incomplete information with learning. This table shows outcomes using two parameter setups. $IV_{ATM,Short\text{-}T}$ is defined in Figure 1, while $Slope_{Mon}$, $Curv_{Mon}$, $Slope_{Mat}$, and $Curv_{Mon}$ are defined in Table III. The percentage of the simulations with significant statistics of the respective diagnostic tests is reported in parentheses at 10% significance.

Variable	$IV_{ATM,Short\text{-}T}$	$Slope_{Mon}$	$Curv_{Mon}$	$Slope_{Mat}$	$Curv_{Mat}$
			α=5.0		
	Panel A: π=66.7%, ρ=8.9%, σ=5.0%, g_u=8.8%, and g_d=-1.5%				
$IV_{ATM,Short\text{-}T}$	1.00				
	(100.00)				
$Slope_{Mon}$	-0.63	1.00			
	(92.80)	(100.00)			
$Curv_{Mon}$	0.60	-0.65	1.00		
	(86.80)	(92.70)	(100.00)		
$Slope_{Mat}$	-0.98	-0.03	0.38	1.00	
	(100.00)	(27.90)	(76.80)	(100.00)	
$Curv_{Mat}$	0.93	0.00	-0.40	-0.95	1.00
	(99.80)	(26.30)	(81.10)	(99.10)	(100.00)
	Panel B: π=66.7%, ρ=9.6%, σ=30.0%, g_u=9.5%, and g_d=-5.0%				
$IV_{ATM,Short\text{-}T}$	1.00				
	(100.00)				
$Slope_{Mon}$	-0.68	1.00			
	(93.50)	(100.00)			
$Curv_{Mon}$	0.54	-0.56	1.00		
	(89.10)	(93.60)	(100.00)		
$Slope_{Mat}$	-0.21	-0.09	0.18	1.00	
	(67.30)	(27.90)	(66.50)	(100.00)	
$Curv_{Mat}$	0.30	0.06	-0.13	-0.23	1.00
	(72.80)	(19.70)	(57.90)	(85.10)	(100.00)

Table EI
Implied Volatility Polynomial Function with Market Data and in an Economy under Breaks and Incomplete Information with Learning

The table contains coefficients estimates and fitting statistics using equation (E1) with average implied volatilities from the U.S. option market and using the Bayesian learning model with multiple parameter combinations.

	b_0	b_1	b_2	b_3	b_4	b_5	R^2	F Statistic	p-value
	Panel A: π=66.7%, ρ=8.9%, σ=5.0%, g_u=8.8%, and g_d=-1.5%								
α= 0.2	2.70	-4.76	2.21	-0.74	0.20	0.47	0.89	53.84	0.00
α= 0.5	4.12	-7.53	3.52	-0.88	0.13	0.71	0.91	37.70	0.00
α= 5.0	-7.04	14.44	-6.94	-0.32	0.71	-0.68	0.94	71.55	0.00
	Panel B: π=66.7%, ρ=9.6%, σ=30.0%, g_u=9.5%, and g_d=-5.0%								
α= 0.2	2.94	-4.90	2.40	-0.73	0.21	0.48	0.88	49.12	0.00
α= 0.5	4.11	-7.16	3.41	-0.94	0.13	0.72	0.90	36.30	0.00
α= 5.0	-5.54	13.99	-7.03	-0.33	0.72	-0.62	0.93	67.68	0.00
	Market Data								
S&P 500 Options	7.31	-13.55	6.39	0.50	-0.03	0.54	0.85	31.75	0.00
Equity Options	4.60	-8.11	3.92	-0.22	0.05	0.12	0.81	43.61	0.00